



University of HUDDERSFIELD

University of Huddersfield Repository

Asim, Taimoor and Mishra, Rakesh

Computational Fluid Dynamics Based Optimal Design of Hydraulic Capsule Pipelines Transporting Cylindrical Capsules

Original Citation

Asim, Taimoor and Mishra, Rakesh (2016) Computational Fluid Dynamics Based Optimal Design of Hydraulic Capsule Pipelines Transporting Cylindrical Capsules. *Powder Technology*, 295. pp. 180-201. ISSN 0032-5910

This version is available at <http://eprints.hud.ac.uk/id/eprint/27889/>

The University Repository is a digital collection of the research output of the University, available on Open Access. Copyright and Moral Rights for the items on this site are retained by the individual author and/or other copyright owners. Users may access full items free of charge; copies of full text items generally can be reproduced, displayed or performed and given to third parties in any format or medium for personal research or study, educational or not-for-profit purposes without prior permission or charge, provided:

- The authors, title and full bibliographic details is credited in any copy;
- A hyperlink and/or URL is included for the original metadata page; and
- The content is not changed in any way.

For more information, including our policy and submission procedure, please contact the Repository Team at: E.mailbox@hud.ac.uk.

<http://eprints.hud.ac.uk/>

COMPUTATIONAL FLUID DYNAMICS BASED OPTIMAL DESIGN OF HYDRAULIC CAPSULE PIPELINES TRANSPORTING CYLINDRICAL CAPSULES

Taimoor Asim^{*1} and Rakesh Mishra²

^{1,2} School of Computing & Engineering

University of Huddersfield, Queensgate, Huddersfield HD1 3DH, UK

¹t.asim@hud.ac.uk, ²r.mishra@hud.ac.uk

Abstract

Rapid depletion of energy resources has immensely affected the transportation sector, where the cargo transportation prices are rising considerably each year. Efforts have been made to develop newer modes of cargo transportation worldwide that are both economical and efficient for a long time. One such mode is the use of energy contained within fluids that flows in the pipelines for transportation of bulk solids. After appropriate modifications to these pipelines, bulk solids can be transported from one location to another very effectively. Solid material can be stored in cylindrical containers (commonly known as capsules), which can then be transported, either singly or in a train through the pipeline. Both the local flow characteristics and global performance parameters associated with such pipelines need careful investigation for economical and efficient system design. Published literature is severely limited in establishing the effects local flow features on system characteristics of Hydraulic Capsule Pipelines (HCPs). The present study focuses on using a well validated Computational Fluid Dynamics (CFD) tool to numerically simulate the solid-liquid mixture flow in HCPs, installed both on-shore and off-shore, along-with the pipe bends. Local static pressure fields have been discussed in detail for a wide range of geometrical and flow related parameters associated with the capsules and the pipelines. Numerical predictions have been used to develop novel semi-empirical prediction models for pressure drop in HCPs, which have then been embedded into a pipeline optimisation methodology that is based on Least-Cost Principle. This novel optimisation methodology that has been developed for HCPs is both robust and user-friendly.

Keywords: Computational Fluid Dynamics (CFD), Hydraulic Capsule Pipeline (HCP), Discrete Phase Modelling (DPM), Particle-Particle Interaction, Least-Cost Principle

1. Introduction

Pipelines are an integral part of various industries throughout the world. The development of pipelines can be broadly categorised into three types:

- First Generation (Single Phase Flow Pipelines)
- Second Generation (Multi-phase Flow Pipelines)
- Third Generation Pipelines (both Pneumatic and Hydraulic Capsule pipelines)

The third generation of pipelines comprises of the transportation of Capsules through pipelines. These capsules are hollow containers filled with minerals, ores etc. In some cases, the material that needs to be transported is itself given the shape of the capsule. The shape of the capsules is normally cylindrical and in some cases wheels are attached to the capsules in order to overcome the static friction between the capsules and the pipe wall because of a larger contact area in the former as compared to cylindrical capsules with wheels.

There are primarily two different types of pipelines i.e. on-shore and off-shore. On-shore pipelines comprise primarily of horizontal pipes, while off-shore pipelines consist of vertical

* Corresponding Author
Tel.: +44 1484 472323

pipes. Furthermore, pipe fittings, such as pipe bends etc., are an integral part of any piping system. For an effective capsule system design interdependence of a large number of local and global variables needs to be established, as this information is not available in literature. Hence, in order to cover a wide range of flow conditions for the analysis of HCPs, both horizontal and vertical pipes transporting cylindrical capsules have been considered for numerical analysis supported by experimental investigations in the present study. Furthermore, a variety of different pipe bends have also been investigated for the flow of cylindrical capsules, such as horizontal-to-horizontal and horizontal-to-vertical bends. After carrying out detailed numerical analysis at component-level, a system-level optimisation study has been carried out in order to optimally design HCPs based on Least-Cost Principle. In the following sections a review of important research works carried out regarding various components of a capsule pipeline system is presented.

1.1 Horizontal HCPs transporting Cylindrical Capsules

There are a large number of geometric, fluid and flow parameters that affect the flow characteristics in a capsule pipeline. Charles [1] conducted an analytical study on the flow of a cylindrical capsule with density equal to that of its carrier fluid. An analytical expression for the velocity of the capsule and for the pressure drop in the pipeline has been presented. The velocity of the capsule and the pressure drop has been assumed to be a function of the diameter ratio 'k' only. The range of investigations is limited to a single cylindrical capsule without considering the effects of the length of the capsule as well as other geometric and flow parameters on the capsule velocity and the pressure drop. Ellis [2] carried out experimental studies on the flow of an equi-density cylindrical capsule in a hydraulic pipe. From dimensional analysis, it was found out that the velocity of the capsule depends on the diameter ratio of capsule-to-pipe and the average flow velocity. In this investigation, the diameter ratio was varied from 0.39 to 0.69, and the average flow velocity of the carrier fluid was varied from 1m/s to 3.7 m/s. It was established in this investigation that the capsule velocity was a function of diameter ratio of the capsule as well as the average flow velocity. Newton et. al. [3] conducted perhaps the first numerical investigation on the flow of a cylindrical capsule in a pipeline. The range of investigations has been kept the same as Ellis [2] with a difference that the capsule length-to-diameter ratio has been varied from 1 to 20. The results presented focused on the capsule velocity and the pressure drop within the pipe. However, the flow has been considered to be laminar, which severely limits the practical application of the study conducted. Kroonenberg [4] developed a mathematical model for the prediction of a cylindrical capsule's velocity and the pressure drop within the pipeline. The velocity field within the pipe has also been investigated however, the actual velocity profiles in the pipe, and in the region between the capsule and the pipe wall, have been neglected, and only mean velocities have been taken into account. This assumption, let alone the other assumptions that have been considered, makes it limited in its usefulness for practical application. This is because the velocity profiles in the pipe, and in the annulus region between the capsule and the pipe wall, have a great impact on the flow behaviour within HCPs. The acceleration of the flow in the annulus, and the presence of the wake region downstream of the cylindrical capsule, have significant implications on the calculation of capsule velocities and pressure drop within the pipeline. Tomita et. al. [5] carried out numerical analysis of the flow of a single cylindrical capsule in a hydraulic pipeline. The study focuses on the velocity and the trajectory of the capsule in the pipe. The capsule has been considered as a point mass in this study. A limited discussion on the velocity and pressure distribution in the vicinity of the capsule has been included. Wheels have been assumed to be attached to the capsule in order to keep the capsule at the centre of the pipeline. Tomita et. al. [6] extended their work by taking into account the flow of a train

of cylindrical capsules, where the spacing between the capsules has been kept variable. A fully developed co-axial flow in the annulus between the capsule and the pipe wall has been assumed. The focus of the study is on the investigation regarding the trajectory and the velocity of the capsules in the pipeline based on variables representing the fluid pressures acting on the front and rear faces of the capsule, the capsule velocity in the radial direction and the coordinates of the capsule. The analysis makes use of the loss coefficient of an abrupt contraction within the pipeline. Lenau et. al. [7] extended Tomita et. al.'s work to develop a numerical model in which the cylindrical capsules have been considered both elastic and rigid bodies respectively. The capsule velocity and trajectory have been found out at node points. Limited discussion on the pressure and velocity distributions has been included. However, the study is limited to the flow of a single cylindrical capsule. Khalil et. al. [8] carried out numerical analysis on the flow of a single long cylindrical capsule in a pipeline. The range of investigations has been limited to k (capsule-to-pipe diameter ratio) of 0.8 to 0.9. A comparison of various turbulence models has been presented. Velocity profiles and pressure drop calculations have been recorded in detail.

Ellis et. al. [9] carried out experimental investigations on the flow of heavy density cylindrical capsules. The study primarily focuses on the pressure drop calculations and power requirements for the pipeline. Jan et. al. [10] carried out experimental investigations on the flow of heavy density cylindrical capsules in an HCP. The range of capsule-to-pipe diameter ratio considered was 0.7 to 0.95, whereas the average flow velocity was kept at 8m/sec. The discussion on the results obtained for the holdup has been limited to the effects of capsule-to-pipe diameter ratios. Ellis et. al. [11] carried out experimental investigations on the flow of heavy density cylindrical capsules in a hydraulic pipeline, where the capsule-to-pipe diameter ratio was varied from 0.39 to 0.89, whereas the average flow velocity varied between 1m/sec and 3.5m/sec. The discussion on the results obtained for the capsule velocities, has been limited to the effects of capsule-to-pipe diameter ratio and average flow velocities on capsule velocity. Kruyer et. al. [12] carried out analytical investigation on the flow of heavy-density cylindrical capsules in laminar flow of water. Detailed analysis on the capsule velocity and pressure drop has been presented. The developed model has been extended to cover turbulent flow as well. Agarwal [13] carried out experimental investigations on the flow of heavy density cylindrical capsules in a hydraulic pipeline, where the capsule-to-pipe diameter ratio was varied from 0.5 to 0.9, whereas the average flow velocity varied between 1.4m/sec and 2.96m/sec. The discussion on the results, obtained for the capsule velocities, focuses primarily on the velocity ratio. Furthermore, Barthes-Biesel et al. [14-15] have numerically studied the motion of deformable capsules as well.

The published literature is limited in terms of the range of flow velocities, capsule diameters, concentration of the capsules, pressure drop considerations and detailed analysis of the pressure distribution within these pipelines. Most concerning is the lack of information about local flow features that has prevented development of robust methods for the design of capsule pipelines. Hence, there is a need for better understanding of the flow structure within horizontal pipelines transporting cylindrical capsules. Furthermore, a wider range of investigations are required in order to built-up an adequate database for accurate analysis and design of horizontal pipelines transporting cylindrical capsules. A well-validated numerical setup can be used to generate data needed for the design with much less effort as compared to extensive experimental programme which may be limited in scope and analysis.

1.2 Vertical HCPs transporting Cylindrical Capsules

Chow [16] carried out extensive investigations on the flow of equi-density cylindrical capsules in a vertical pipeline, where the capsule-to-pipe diameter ratio was 0.5 to 0.9, whereas the average flow velocity varied between 1m/sec and 4m/sec. The range of capsule

lengths considered was $1d$ to $14d$, d being the diameter of the capsule. A detailed analysis has been presented regarding the velocity of the capsules and the pressure drop within the pipeline and the semi-empirical expressions for these variables have been developed. Hwang et. al. [17] carried out both analytical and experimental investigations on the flow of heavy-density cylindrical capsules in a vertical pipeline, where the capsule-to-pipe diameter ratio was 0.5 to 0.9. The primary focus of the study was to find the overall efficiency of the capsule transporting system, in terms of energy loss or pressure drop. It has been reported that the best value of capsule-to-pipe diameter ratio, which corresponds to the maximum efficiency of the system, is $2/3$ or 0.66. Furthermore, it has been reported that the length of the capsule has little influence on the efficiency of the system. Latta et. al. [18] carried out experimental studies on the flow of heavy-density cylindrical capsules in a vertical pipe, where the capsule-to-pipe diameter ratio was varied from 0.5 to 0.9, between average flow velocities of 1m/sec and 4m/sec. The range of capsule lengths considered was $1d$ to $14d$. A detailed analysis of the capsule velocities and the pressure drop within the pipeline has been presented. Motoyoshi [19] conducted experimental studies on the flow of heavy-density cylindrical capsules in inclined and vertical pipelines, where the capsule-to-pipe diameter ratio was 0.5 to, at an average flow velocity of 0.9m/sec. The range of capsule lengths considered was from $2d$ to $10d$. The study focuses on the energy loss in the systems. It has been reported that capsules with lower Lc/d have lower energy loss associated with them. Furthermore, the variations in energy loss are non-linear with respect to the angle of inclination of the pipeline.

Akira et. al. [20] conducted both analytical and experimental studies on the flow of cylindrical capsules in a vertical pipeline, where the capsule-to-pipe diameter ratio was varied from 0.78 to 0.96. The range of specific gravities and capsule lengths considered were from 1.39 to 7.84 and from $1.5d$ to $5d$ respectively. A model for the prediction of the pressure drop (ΔP) across the pipeline, as a function of the Froude number of the capsules, has been developed. Katsuya et. al. [21] conducted analytical and experimental investigations on the flow of cylindrical capsules in a vertical pipeline. A detailed discussion on the flow development in such pipelines has been presented. Furthermore, the drag coefficient of the capsules under varying geometric and flow conditions has been reported. Prabhata et. al. [22] conducted design studies on the flow of cylindrical capsules of various densities (both equal and heavy) in a vertical pipeline. It has been observed that the published literature is severely limited in terms of component level investigations within vertical HCPs. Furthermore, a more in-depth analysis of the flow field within such pipelines is required. Furthermore, a wider range of investigations are required in order to built-up an adequate database for accurate analysis and design of vertical HCPs transporting cylindrical capsules.

1.3 HCP bends transporting Cylindrical Capsules

Vlasak et. al. [23] conducted experimental studies on the flow of heavy-density cylindrical capsules in both horizontal and vertical bends of various radii of curvature. The results presented for the velocity ratio and pressure gradient indicate that the pressure drop in vertical bends is significantly higher as compared to horizontal pipe bends. Furthermore, it has been reported that the radius of curvature of the bend has insignificant effect on the velocity ratio of the capsules. Vlasak et. al. [24] conducted experimental studies on the flow of heavy-density cylindrical capsules in vertical bends, of bend-to-pipe radius ratio of 2, where the length of the capsules was equal to $5d$. The results for the velocity ratio and the pressure gradient have been presented. It has been reported that as the average flow velocity increases within a pipe bend, the holdup also increases. It can be seen that the published literature is severely limited, on the information regarding the complex flow phenomena within HCP bends. Hence, the boundary conditions of capsule velocities, for numerical

analysis, cannot be extracted from the literature presented, and hence the present study uses a novel technique, called Discrete Phase Modelling (DPM), in order to artificially simulate the flow of cylindrical capsules in pipe bends, both horizontal and vertical. Using this method, capsule velocities and trajectories can be calculated, which will serve as boundary conditions for the detailed numerical analysis.

1.4 Design and Optimisation of Solid-Liquid Mixture Flow Pipelines

Polderman [25] reported design rules for hydraulic capsule systems for both on-shore and off-shore applications. Design rules are based on variables such as the pressure drop in the pipeline, Reynolds Number of capsules etc. A general indication towards parameters that might be used for an optimisation model has been given. However, no such optimisation model has been developed, which can be used for designing a pipeline transporting capsules. Morteza et. al. [26] developed an optimisation model for pipelines transporting capsules based on maximum pumping efficiency. Prabhata [27] has developed an optimisation model for sediment transport pipelines based on the least-cost principle. The model assumes the value of the friction factor as the input to the model, strictly limiting its usefulness for commercial applications. Swamee [22] has developed a model for the optimisation of equi-density cylindrical capsules in a hydraulic pipeline. The model is based on least-cost principle. The input to the model is the solid throughput required from the system. The friction factors considered, however, are not representative of the capsule flow in the pipeline, and hence severely limit the practicality of the model. Agarwal et. al. [28] has developed an optimisation model for multi-stage pipelines transporting capsules. The model is based on the principle of least-cost and uses the solid throughput as the input to the model. The model developed is applicable for contacting cylindrical capsules only, occupying the complete length of the pipeline. Furthermore, this optimisation model uses limited parameters for the analysis of HCPs, and considers homogeneous model for pressure drop prediction, which all add-up to restrict the practicability of this optimisation model. Yongbai [29] has developed an optimisation model for hydraulic pipelines based on saving energy sources. The model, however, cannot be used for multi-phase flows. Asim et. al. [30] has extended Agarwal's optimisation model [28] to include the effects of spacing between the capsules. Furthermore, this optimisation model considers a wider range of geometric and flow related variables. However, Asim's optimisation model addresses spherical capsules only. At system-level optimisation of HCPs, only limited works are available which cover a wide range of operating conditions. Hence, this study presents a modified version of Asim's optimisation model, where cylindrical capsules have been considered within the HCP, covering a wide range of operating conditions. The optimisation model developed is based on Least-Cost Principle. The pressure drop prediction models developed in this study from the analysis of horizontal HCPs, vertical HCPs and HCP bends, are all embedded into this optimisation model.

2. Pressure drop considerations in HCPs

The pressure drop in a hydraulic pipeline transporting a fluid can be computed from Darcy Weisbach equation [31]:

$$\Delta P = f \frac{L_p}{D} \frac{1}{2} \rho V^2 \quad (1)$$

where ΔP is the pressure drop across the pipe, f is Darcy's friction factor, L_p is the length of the pipe, D is the diameter of the pipe, ρ is the density of fluid and V is the flow velocity within the pipe. Darcy's equation can be extended to compute pressure drop within HCPs.

This can be achieved by separating the pressure drop within the pipeline due to water alone, and due to capsules only [32]. This can be expressed as:

$$\Delta P_m = k_1 f_w \frac{L_p}{D} \frac{k_2 \rho_w (1-c) k_3 V_{av}^2}{2} + k_4 f_c \frac{L_p}{D} \frac{k_5 \rho_w c k_6 V_{av}^2}{2} \quad (2)$$

where ΔP_m represents the pressure drop across the pipe due to the mixture flow, ρ_w is the density of water, c is the concentration of the solid phase in the mixture, V_{av} is the average flow velocity and the constants $k_1, k_2, k_3, k_4, k_5, k_6$ are the coefficients which relate the friction factor, density and the velocity of both the water and the capsules respectively to that of the mixture. If the effect of the concentration of the solid phase c and the constants $k_1, k_2, k_3, k_4, k_5, k_6$ are represented in friction factor due to water alone (f_w) and friction factor due to capsules only (f_c), then equation (2) can be simplified as:

$$f_w = f(c, k_1, k_2, k_3) \quad (3)$$

$$f_c = f(c, k_4, k_5, k_6) \quad (4)$$

Hence, the pressure drop in an HCP can be computed as:

$$\Delta P_m = f_w \frac{L_p}{D} \frac{\rho_w V_{av}^2}{2} + f_c \frac{L_p}{D} \frac{\rho_w V_{av}^2}{2} \quad (5)$$

Equation (5) is valid for the horizontal HCPs. This equation can be extended further to include the elevation effects as:

$$\Delta P_m = f_w \frac{L_p}{D} \frac{\rho_w V_{av}^2}{2} + f_c \frac{L_p}{D} \frac{\rho_w V_{av}^2}{2} + \rho_w g \Delta h_w \quad (6)$$

where g is the gravitational acceleration and Δh_w is the elevation of the water column. Hence, equations (5) and (6) represent the major losses in HCPs. In order to compute the minor losses within HCPs (both horizontal and vertical); the following expressions have been derived:

$$K_l = \frac{\Delta P}{\frac{1}{2} \rho V^2} \quad (7)$$

$$\Delta P_m = K_{lw} \frac{n \rho_w V_{av}^2}{2} + K_{lc} \frac{n \rho_w V_{av}^2}{2} \quad (8)$$

$$\Delta P_m = K_{lw} \frac{n \rho_w V_{av}^2}{2} + K_{lc} \frac{n \rho_w V_{av}^2}{2} + \rho_w g \Delta h_w \quad (9)$$

where K_{lw} represent the loss coefficient of the bend due to water, K_{lc} is the loss coefficient of the bend due to capsule and n is the number of bends attached to the pipeline. Hence, equations (8) and (9) include the minor losses within HCPs. f_w and f_c in equations (3) and (4) can be determined using either experimental or well verified numerical methods, where numerical methods can further provide useful information regarding the flow structure within HCPs rapidly. In the present study, these coefficients have been computed using advanced CFD based techniques. The next section provides detailed information regarding the CFD setup that has been used in the present study for the analysis of HCPs transporting cylindrical capsules.

3. Geometrical Configurations of the HCP

The geometry of the HCP has been created using a commercial CFD package called ANSYS-Fluent. The HCP's numerical model comprises of three sections i.e. an inlet pipe, a test section and an outlet pipe, where the lengths of these three sections are 5m, 1m and 1m respectively, as shown in figure 1. A 5m long inlet pipe is used in order to allow the flow to become fully developed [33]. A 1m long outlet pipe has been used in order to fulfil numerical solver's requirements i.e. the boundaries of the flow domain should be far away from the area of interest, which is the test section in the present case. The test section is similar to that of Ulusarslan et. al. with a 0.1m internal diameter [34]. The pipe surface has been considered to be hydrodynamically smooth, with an absolute roughness constant (ϵ) of zero. It has been noticed by Ulusarslan et al. that there has been no significant change in the spacing between the capsules when velocity changes at a particular concentration.

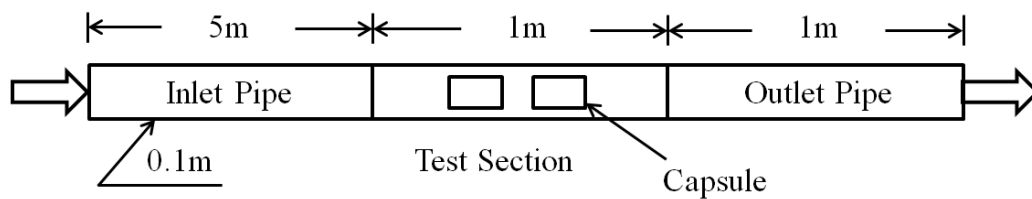


Figure 1 Schematic of the horizontal HCP

Two of the industrially most widely used 90° HCP bends of bend-to-pipe radius ratios of 4 and 8 have also been numerically created and analysed in the present study, as shown in figure 2 [35].

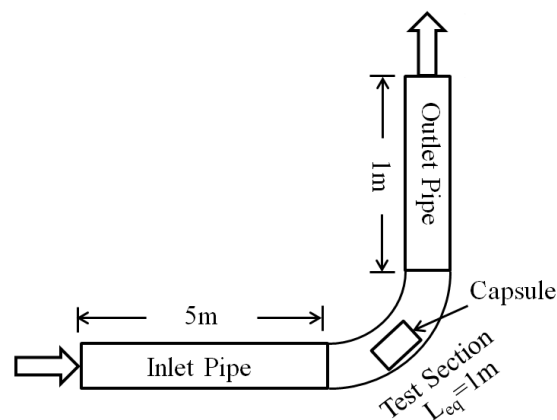


Figure 2 Schematic of an HCP Bend

The concept of hybrid meshing has been incorporated for the meshing of the flow domain. Two different meshes used i.e. a structured hexahedral mesh for the Inlet and Outlet pipes, while an unstructured tetrahedral mesh for the Test section due to the presence of capsule/s. Two different meshes with 1000,000 and 2000,000 mesh elements had been chosen for mesh independence testing. The results obtained, shown in table 1, depict that the difference in the pressure drop across the HCP is less than 1% from the two meshes under consideration. It can therefore be concluded that the mesh with one million elements is capable of accurately predicting the flow features, and hence has been chosen for further analysis. It has been ensured that the y^+ value is under 10 for the capsules and the pipe wall, in order to resolve the boundary layer with reasonable accuracy.

Table 1. Mesh Independence Results

Number of Mesh Elements	Pressure at Inlet	Pressure at Outlet	Pressure Drop per unit Length	Difference in Pressure Drops
	(Pa)	(Pa)	(Pa/m)	(%)
1 million	11163	401	10762	0.75
2 million	11265	584	10681	

4. Boundary Conditions

The boundary types and conditions that have been specified are listed in table 2. A practical range of inlet flow velocities have been considered here, corresponding to a 100mm diameter pipeline, as considered by many other researchers [1, 2, 9, 18, 30, 32]. The pressure at the inlet boundary has been numerically computed by the solver by specifying pressure at the outlet boundary. Furthermore, appropriate boundary conditions have been specified to the pipe wall and the different faces of the capsule/s.

Table 2 Boundary Conditions

Boundary Name	Boundary Type	Boundary Conditions
Inlet to the Pipe	Velocity Inlet	1–4m/sec
Outlet of the Pipe	Pressure Outlet	0Pa(g)
Wall of the Pipe	Stationary Wall	No-Slip
Capsules	Moving Walls	From Literature/experiments

The details of capsule/s velocities are discussed in the following sub-sections.

4.1 Capsule Velocity in Horizontal HCPs

Charles [1] presented a theoretical analysis of the concentric flow of a cylindrical capsule with density of the capsule equal to that of water. The model developed for the prediction of the capsule's velocity in the turbulent flow within a horizontal pipeline, shows that the holdup (V_c/V_{av}) for the capsule depends on the capsule to pipe diameter ratio k . The velocity of the capsule has been represented by the following expression:

$$V_c = \left[\frac{1}{\left\{ \frac{7}{4}k(1-k) + \frac{49}{60}(1-k^2) + k^2 \right\}} \right] * V_{av} \quad (10)$$

where V_c is the capsule velocity, k is the capsule-to-pipe diameter ratio and V_{av} is the average flow velocity. Furthermore, Ellis [9] conducted experimental investigations on the transport of a cylindrical capsule made of aluminium with a specific gravity of 2.7. The experimental data has been analysed using multiple variable regression. Using the coefficients obtained from multiple variable regression analysis, the following expression for the velocity of the capsule has been obtained:

$$V_c = (0.77 * V_{av}) - \left(0.008 * \frac{L_c}{d} * V_{av} \right) + (0.302 * k * V_{av}) \quad (11)$$

The velocities of the capsule calculated using the equation above and obtained from the experimental data obtained in the present study have been plotted. It can be clearly seen in figure 3 that the calculated velocities of the capsules are in good agreement with the

experimental data and more than 80% of the data lies within $\pm 5\%$ error bound of the equation above.

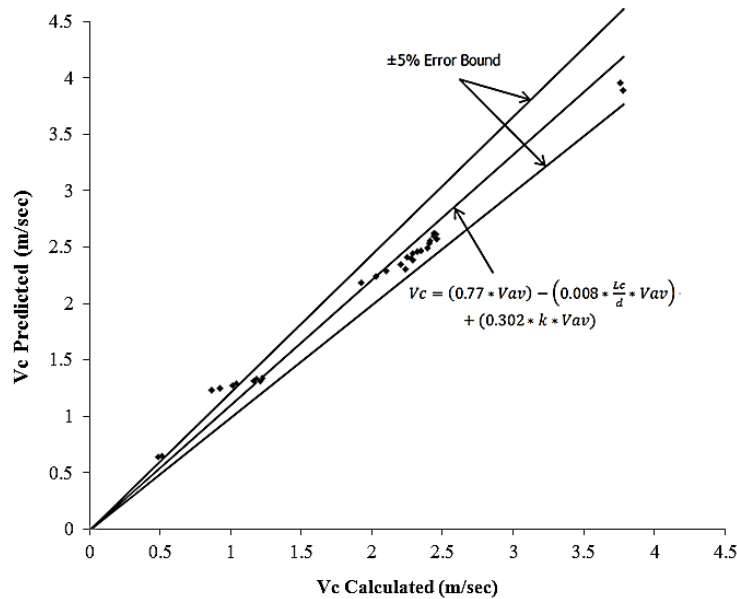


Figure 3 Comparison between computed and predicted capsule velocities

A 50mm HCP flow loop setup has been developed and the capsule velocities have been recorded for various flow velocities and capsule sizes. It has been observed that the experimentally recorded capsule velocities are in close agreement with the one calculated through the use of equation (11). Details of the experimental setup are included in section 6.

4.2 Capsule Velocity in Vertical HCPs

Latto [18] reports the velocity of the cylindrical capsules with density equal to that of water as:

$$Vc = \frac{vav}{k^{0.128}} * \left(\frac{Lc}{d}\right)^{0.128} \quad (12)$$

Using the above equation, the velocity of the capsules, for different cases under investigation, has been calculated. Furthermore, Latto [18] proposed an equation for the velocity of the cylindrical capsules with density greater than that of water as:

$$Vc = \frac{vav}{k^{0.128}} \left(\frac{Lc}{d}\right)^{0.128} - \frac{\left(\sqrt{2gD\left(\frac{Lc}{d}\right)^{(s-1)}(1-k^2)\left(1-\frac{1}{s}\right)^{0.05}}\right)}{k^{0.128}} \quad (13)$$

Using the above equation, the velocity of the capsules, for different cases under investigation, has been calculated.

4.3 Capsule Velocity in Pipe Bends

Discrete Phase Modelling (DPM) has been used in the present study in order to predict the velocity of cylindrical capsule/s in HCPs. DPM solves transport equations for the continuous phase, i.e. water in case of hydraulic capsule bends. It also allows simulating a discrete second phase in a Lagrangian frame [36]. This second phase consists of cylindrical particles (having same size as that of the capsules) dispersed in the continuous phase. DPM computes the trajectories of these discrete phase entities. The coupling between the phases and its impact on both the discrete phase velocities and trajectories, and the continuous phase flow

has been included in the present study. The discrete phase in the DPM is defined by defining the initial position and size of the capsules. These initial conditions, along with the inputs defining the physical properties of the discrete phase (capsule), are used to initiate trajectory and velocity calculations. The trajectory and velocity calculations are based on the force balance on the capsule. The trajectory of a discrete phase particle is predicted by integrating the force balance on the particle, which is recorded in a Lagrangian reference frame. This force balance equates the particle inertia with the forces acting on the particle. The velocity of cylindrical capsules is assumed to be a function of capsule's location within the bend. In order to investigate the likely influence of the angular position of cylindrical capsules within HCP bends, detailed analysis has been carried out at six equally spaced angular positions of 0°, 18°, 36°, 54°, 72° and 90° to cover a wide range of analysis. After conducting some preliminary investigations, it has been observed that the pressure drop in a pipe bend transporting cylindrical capsules is almost independent of the angular position of the capsule, where the density of the capsules is equal to that of water. However, the pressure drop is significantly different at different locations in case of the flow of heavy-density cylindrical capsules in pipe bends. Hence, an average pressure drop has been considered for the analysis of the flow of heavy-density cylindrical capsules in pipe bends. The average percentage error in pressure drop estimation has been computed to be less than 5%.

5. Scope of Numerical Investigations

As there are a large number of geometric and flow related variables associated with the flow of cylindrical capsules in pipelines, a Full Factorial based Design of Experiments (DoE) has been employed in the present study to determine the possible practical combinations of these parameters. Minitab 17 Statistical Software has been used in the present study to carry out Full Factorial based DoE studies, where a practical range of different parameters has been specified. The factors/parameters considered for the flow of cylindrical capsules in HCPs, along-with their levels, have been summarised in table 3. It can be seen that the current investigations not only consider the flow of a single capsule in HCPs, but a capsule train as well, where the train consists of two cylindrical capsules in the present study. Three different lengths of the capsules have been considered i.e. 1d, 3d and 5d, d being the diameter of the capsules. Capsule-to-pipe diameters ratios of 0.5 and 0.7 have been considered in the present study, while average flow velocities of upto 4m/sec have been employed. The spacing between the capsules, in a capsule train, has been varied as 1d, 3d and 5d. Furthermore, bend-to-pipe radius ratios of 4 and 8, representing the most common industrial pipe bends, have been used in HCPs. Moreover, both equi-density and heavy-density cylindrical capsules have been considered in the present study.

Table 3 Factors and Levels for Full Factorial Design of an HCP

Factor	Level 1	Level 2	Level 3	Level 4
N/Lp	1	2	N/A	N/A
Lc	1d	3d	5d	N/A
k	0.5	0.7	N/A	N/A
V _{av}	1	2	3	4
Sc	1d	3d	5d	N/A
R/r	4	8	N/A	N/A
s	1	2.7	N/A	N/A

The resulting numbers of numerical simulations, which are equal to 373, have been performed, and the pressure drop per unit length of the pipeline has been recorded for each simulation. Novel semi-empirical prediction models, similar to equations (5-6 and 8-9), have

then been developed for the friction factor/s and loss coefficient/s of capsule/s. These semi-empirical prediction models have then been embedded into the least-cost principle based optimisation methodology developed in the present study for cylindrical capsules.

6. Experimental Setup and Instrumentation

A flow loop having a test section of 50mm diameter pipeline has been developed in order to experimentally verify the boundary conditions i.e. the capsule velocity within a horizontal pipeline, so that numerical simulations represent realistic pipe flow. The pipes and the fittings used in the construction of the flow loop are made of impact resistant unplasticised polyvinyl chloride (PVC), where the maximum operating pressure for the pipes and fittings is 16bar. Two cylindrical capsules of capsule-to-pipe diameter ratios of 0.5 and 0.7, and length equal to that of capsule's diameter, have been cut out of an aluminium rod. A 1m x 1m x 1m water tank has been connected to Wilo CronoLine-IL 100/210-37/2 centrifugal pump by a PN16 flange (according to EN 1092-2). The centrifugal pump has a maximum operating pressure of 16bar at maximum pumping fluid temperature of 120°C and at a maximum ambient temperature of 40°C. The rated power of pump's motor is 37kW at 2900rpm, where the efficiency of the motor ranges from 92% to 93.7%, whereas the minimum efficiency index (MEI) of the pump is ≥ 0.4 . Pump's flow rate has been varied to get appropriate V_{av} values. This is achieved through the use of an 11kW Siemens Optima Pump Test Rig which has a flexible and sophisticated control system, integrating a programmable logic controller and human interface to enable specific timing and control setting functions to automatically operate pump's rotational speed. The centrifugal pump is connected to the capsule injection system via a digital turbine flow meter that has an accuracy of $\pm 3\%$ of reading and a pressure rating of 225psi at 22.7°F. The operating temperature of the flow meter is 32°C to 60°C with a flow range of 76 to 760ltrs/min. The capsule injection system constitutes the secondary loop within the primary flow loop. The capsule injection system, as shown in figure 4, comprises of a number of ball valves to restrict water flow in certain sections of the flow loop, while a pneumatically controlled knife gate valve is installed as a barrier between the capsule/s and the water flow in the primary loop. The primary loop consists of a 1.75m long horizontal pipe which serves as the test section for recording capsule velocity.

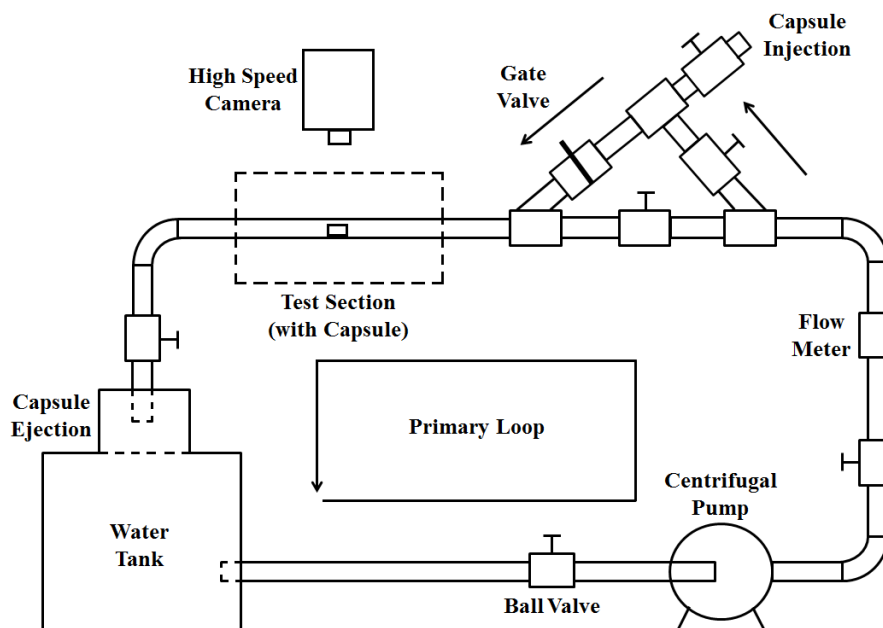


Figure 4 Test setup for capsule flow

Once the capsule is fed into the capsule injection system, while the secondary loop is shut, the knife gate valve is opened, leading the capsule into the primary loop. A high speed camera, Photron FASTCAM SA3, is mounted perpendicularly at the same level as the test section. The high speed camera has a maximum frame rate of 120,000fps. The frame rate used for recording capsule velocity has been set at 1000fps, with 1024x512 image resolution. A measuring scale has been used alongside the test section in order to evaluate capsule velocity by using time of travel measurements from the camera. The high speed camera is connected to a PC via a 1000BASE-T Gigabit Ethernet Interface and a LAN cable beyond CAT5e standard. The capsule is then collected on the top of the water tank by a capsule ejection mechanism, while the water is drained into the tank. Figure 5 depicts two instances where a capsule of capsule-to-pipe diameter ratio of 0.7 is being transported by water at an average flow velocity of 3.06m/sec within the test section. It can be seen that as the capsule is heavy-density, it travels/slides along the bottom wall of the pipe, where its trajectory remains constant throughout the test section.

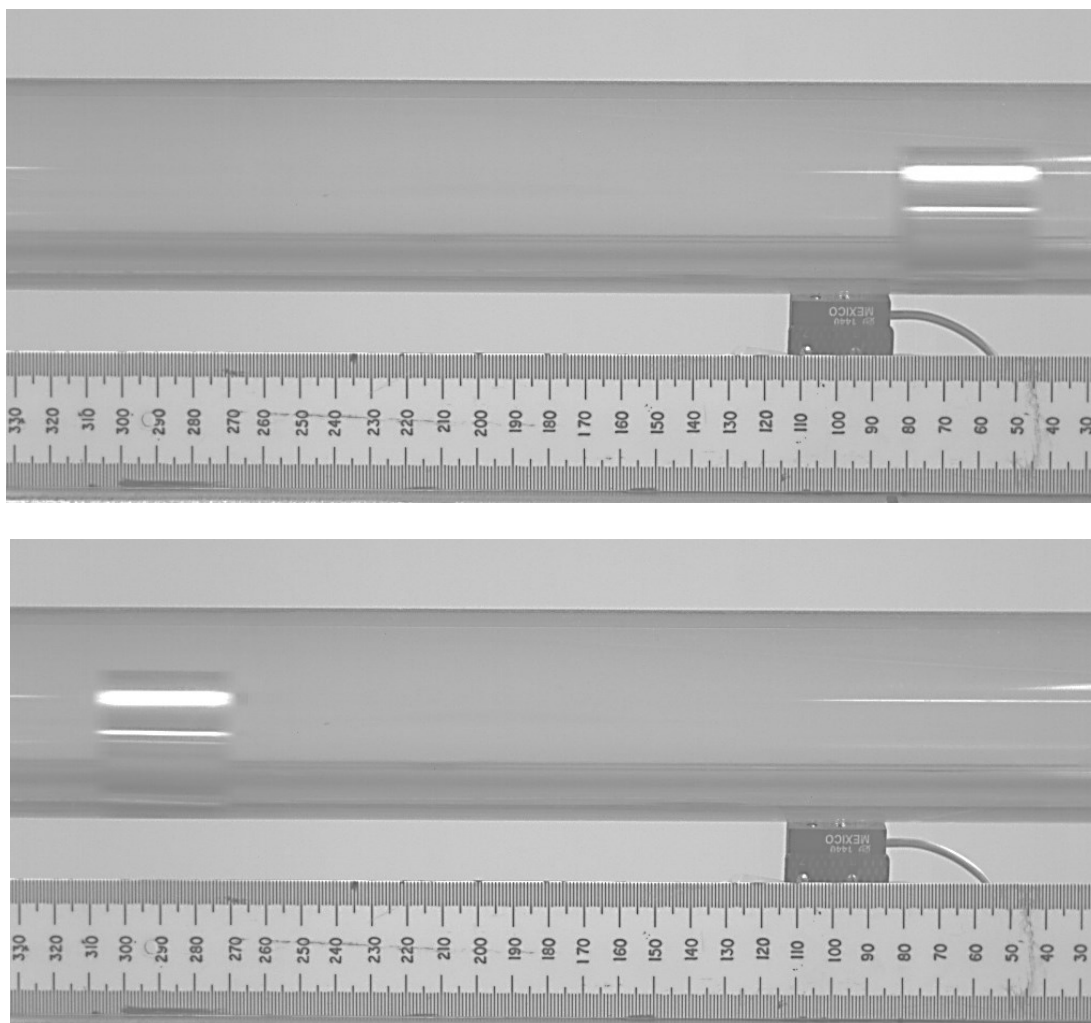


Figure 5 Flow path of a heavy-density cylindrical capsule of $k=0.7$ and $L_c=1d$ at $V_{av}=3.06$ at two different instances

Table 4 shows comparison between equation (11) and the experimental findings of this study. It can be clearly seen that both the results are in close agreement at different V_{av} and k values, and hence equation (11) has been used to find out capsule's velocities at other operating conditions as defined in the scope of the present work.

Table 4 Capsule velocity comparison

k	V_{av} (m/sec)	V_c from equation (11) (m/sec)	V_c from experiments (m/sec)	Difference in V_c (%)
0.7	2.18	2.12	2.08	1.89
	3.06	2.97	3.06	3.03
	3.20	3.11	3.19	2.57
0.5	2.18	1.99	2.03	2.01
	3.06	2.79	2.70	3.23
	3.20	2.92	2.85	2.40

7. Verification of CFD results

Numerical predictions need to be verified against the experimental results in order to gain confidence on these predictions. Furthermore, appropriate solver settings, such as boundary conditions, turbulence modelling, gradient and interpolation schemes etc., need to be specified to the numerical simulations for accuracy in predictions. After successful verification of numerical predictions, the same solver settings can then be used for further analysis/investigations. In the present study, verification of CFD predictions regarding the pressure drop within an HCP has been carried out against the experimental results of Ulusarslan [37]. Table 5 summarises the benchmarking parameters used for the verification purposes.

Table 5 Benchmarking parameters

Name/Property	Value/Range/Comment
s	0.87
k	0.8
V_{av}	0.2–1 m/sec
N/Lp	Depending on concentration

Three dimensional Navier-Stokes equations, along-with the continuity equation, have been numerically solved for the turbulent flow of water, with cylindrical capsules waterborne, in a horizontal HCP. Pressure drop predictions from the CFD analysis, across the HCP, have been compared against the experimental results, as shown in figure 6. It can be observed that the CFD predicted pressure drop values are in close agreement with the experimental results, with an average variation of less than 5% for all solid phase concentrations (c). It can thus be concluded that the numerical model considered in the present study represent the physical model of a pipeline transporting cylindrical capsules.

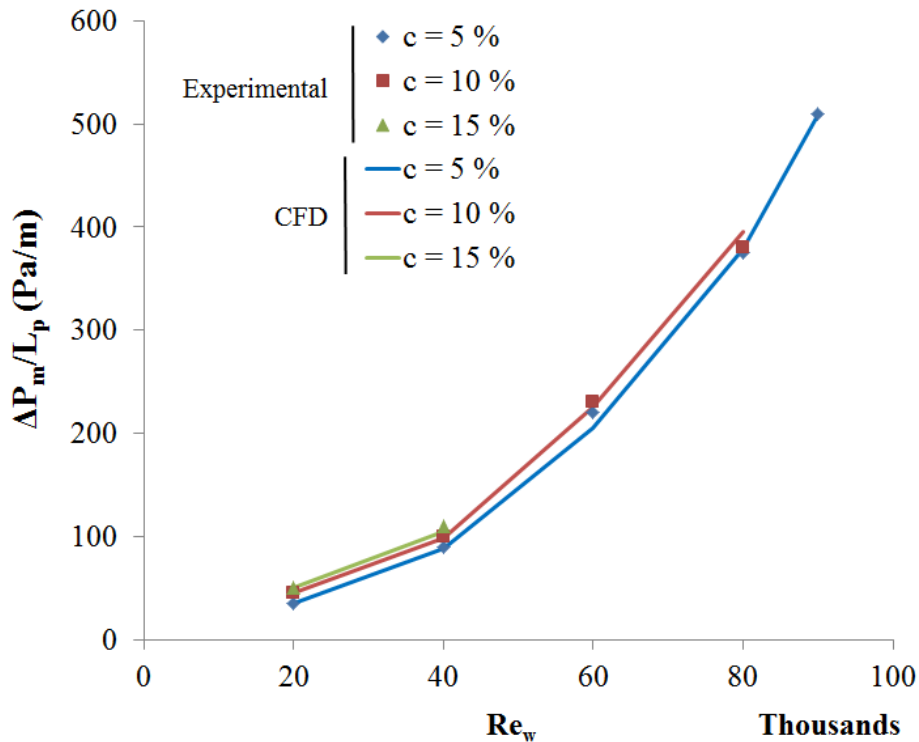


Figure 6 Comparison between CFD predicted and experimentally recorded pressure drop within an HCP

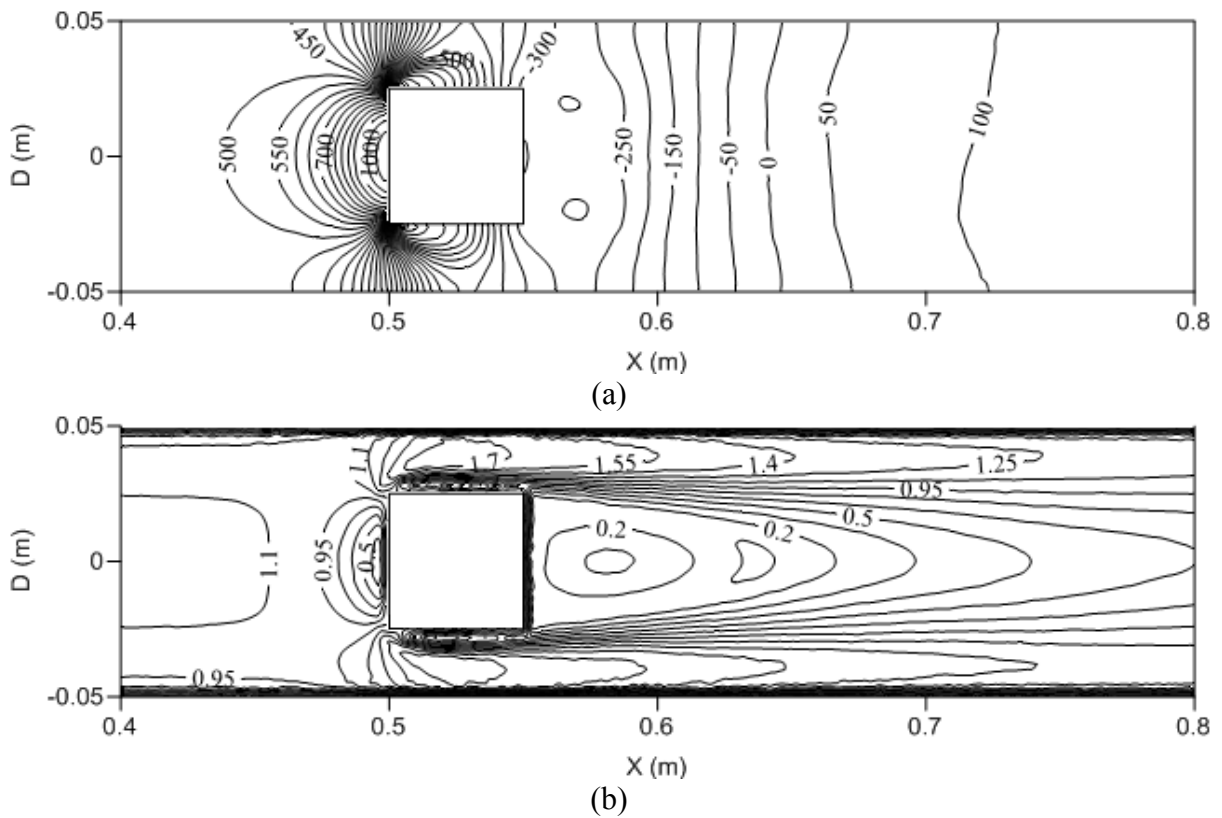
8. Results and Discussion

It has been observed that the local flow features within a capsule pipeline have not been investigated extensively. In the following section the local flow field analysis for the flow of cylindrical capsules in a hydraulic capsule pipeline has been presented. The main focus of these analyses is to explicitly establish dependence of local flow parameters, like pressure, velocity etc., on the global performance parameters, like pressure drop etc. For this purpose, the effects of several geometrical and flow conditions on the local flow features have been obtained numerically. In particular, the effects of capsule concentration within the HCP, capsule size, average flow velocity and specific gravity of the capsules, along-with the effects of pipe inclination and pipe curvature have been enumerated. The predicted results have then been used to develop novel semi-empirical expressions for the pressure drop within HCPs, which in-turn has been embedded into the HCP optimisation methodology developed for the flow of cylindrical capsules in HCPs.

Figure 7 depicts the local variations in the static pressure, velocity and vorticity magnitudes within the test section of the horizontal pipe, transporting a single equi-density cylindrical capsule of capsule-to-pipe diameter ratio of 0.5 at an average flow velocity of 1m/sec. The length of the capsule considered here is equal to the diameter of the capsule. As this is the first case determined through the use of full factorial based DoE studies, and represents a common practical scenario in HCPs, it has been chosen as a general case study, while comparisons have been made to this case in the upcoming sub-sections.

It can be seen in figure 7(a) that the presence of a capsule makes the static pressure distribution highly non-uniform within the HCP, as compared to single phase flow where it is known that static pressure remains constant along the radial direction at a particular pipe cross-section [38]. The pressure gradients are fairly large upstream the capsule. The higher upstream static pressure is due to the difference between the average flow velocity and the capsule velocity. This is associated with reduction in the flow velocity upstream the capsule,

as depicted in figure 7(b). The flow then enters the annulus region between the pipe wall and the capsule. As the cross-sectional area decreases, the flow accelerates, resulting in reduction in the static pressure. The flow, while exiting the annulus region, decelerates, resulting in increase in the static pressure. Here, the shear layers roll-up due to velocity gradient, forming vortices, which are being shed into the wake of the capsule, as depicted in figure 7(c). The vortices shed downstream the capsule grow in size initially, taking their energy from the shear layers, through their trailing jets. This has been observed and explained in more detail by Gharib et. al. [39-42]. Once enough amount of energy has been transferred to the vortices, they detach themselves from the shear layers and travel further downstream, constantly expanding in size and dissipating their energy, leading to their eventual decay. The flow then recovers rapidly from the effects of the presence of capsule within the pipe and the static pressure recovers to some extent. This is associated with further reduction in the vorticity.



In order to quantitatively analyse the effects of the presence of a single equi-density cylindrical capsule within a horizontal pipe, the drag force acting on the capsule has been computed in non-dimensional form. The drag coefficient has been found to be 2.169. The drag coefficient value is well within the expected range, as mentioned in the works of Feng et. al. [43] and Yanaida et. al. [21].

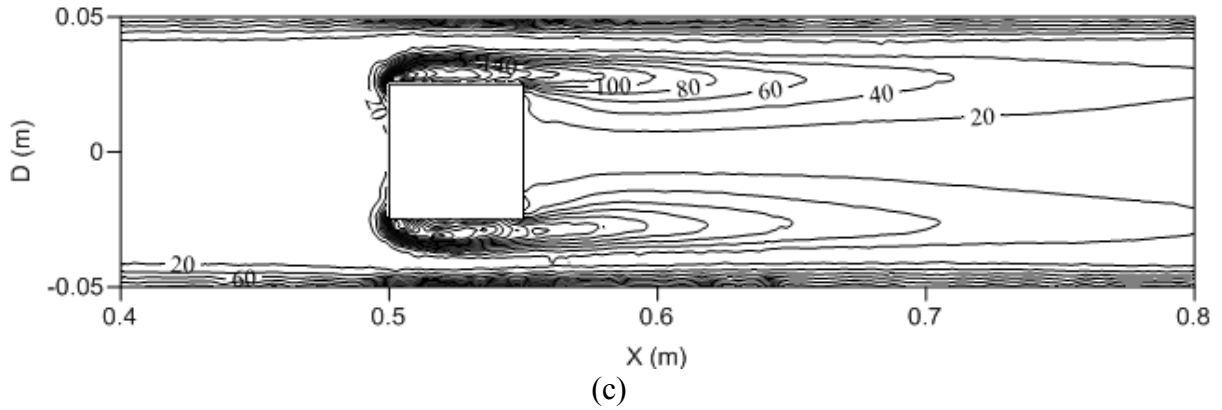


Figure 7 Flow fields within a horizontal HCP transporting a single equi-density cylindrical capsule of $k=0.5$ and $L_c=1d$ at $V_{av}=1\text{m/sec}$ (a) Static pressure (Pa) (b) Velocity magnitude (m/sec) (c) Vorticity magnitude (/sec)

The drag coefficient is closely related to the pressure drop due to the presence of capsules in HCPs, as discussed in detail by Liu [44]. In order to inter-relate the local flow characteristics with the drag coefficient of the capsule, a novel parameter has been developed that indicates the resultant pressure force acting on the capsule because of the relative velocity between the capsule and the flow. Computing the local static pressure on the front and rear ends of the capsule and subtracting the effects of the main flow within the pipeline i.e. at freestream location, the authors define a parameter α that represents the non-uniformity in pressure distribution caused by the presence of the capsule. The value of α has been computed as:

$$\alpha = \frac{P_F - P_\infty}{P_\infty - P_R} \quad (14)$$

where P_F and P_R are static pressures on the front and rear ends of the cylindrical capsule, while P_∞ is the static pressure on a cross-sectional area at freestream/undisturbed location upstream the capsule. It can be noticed that as P_F is always higher than P_∞ , while P_R is expected to be negative in most cases of HCPs, α is expected to be a positive number in most scenarios. Furthermore, α is inversely proportional to the pressure drop i.e. when the pressure drop increases, the wake region of the capsule is expected to be bigger, indicating more losses and lower P_R values, hence, the denominator of equation (14) will be a higher value, and α will be lower. The value of α in the present case is 0.466.

The effect of the presence of an equi-density cylindrical capsule, on the pressure drop across the HCP, has been depicted in figure 8. The y-axis of the figure represents non-dimensional pressure drop across a given length of the pipeline, specifying values between particular regions. These regions have been chosen to be between (a) $2d$ and $1d$ upstream the capsule, (b) $1d$ and the front face of the capsule, (c) the front and the rear faces of the capsule, (d) rear face of the capsule and $1d$ downstream it, (e) $1d$ and $3d$ downstream the capsule, (f) $3d$ and $5d$ downstream the capsule and (g) $5d$ and $3d$ downstream the capsule. It can be seen that the pressure drop between the aforementioned cross-sectional areas within a hydraulic pipeline remains constant, and is shown as a straight line in the figure. However, when a cylindrical capsule is introduced into the pipeline, the pressure drop varies in the region around the capsule. It can be noticed that the pressure drop between the locations that are two and one diameters of the capsule upstream of the capsule ($2d$ and $1d$ respectively), is equal to that of a hydraulic pipeline. Hence, the effect of the capsule is not felt in this region. However, the pressure drop increases significantly between the front face of the capsule (F) and a location that is one diameter of the capsule upstream of the capsule. As this point in the figure attains

the highest pressure drop value, it can be concluded that the most pressure drop due to the presence of capsule occurs in the area immediately in and around the capsule flow space. The pressure drop keeps on decreasing downstream the capsule until it can be seen that between locations that are 5 and 10 diameters of the capsule downstream the capsule (5d and 10d respectively), the pressure drop across the HCP is the same as the pressure drop offered by water only. Hence, the effect of the capsule is felt 1d upstream the capsule to 5d downstream the capsule. α of the HCP has been calculated to be 414Pa(g) as compared to 92Pa(g) in case of water flow only. Hence, friction factors f_w and f_c have been computed to be 0.0184 and 0.0645 respectively, clearly showing that the pressure drop in case of an HCP is significantly higher than a hydraulic pipeline. The values of f_w and f_c computed here, accommodate the changes in the parameters discussed in equations (3) and (4), and hence can be used in order to develop novel semi-empirical prediction models for the pressure drop across HCPs.

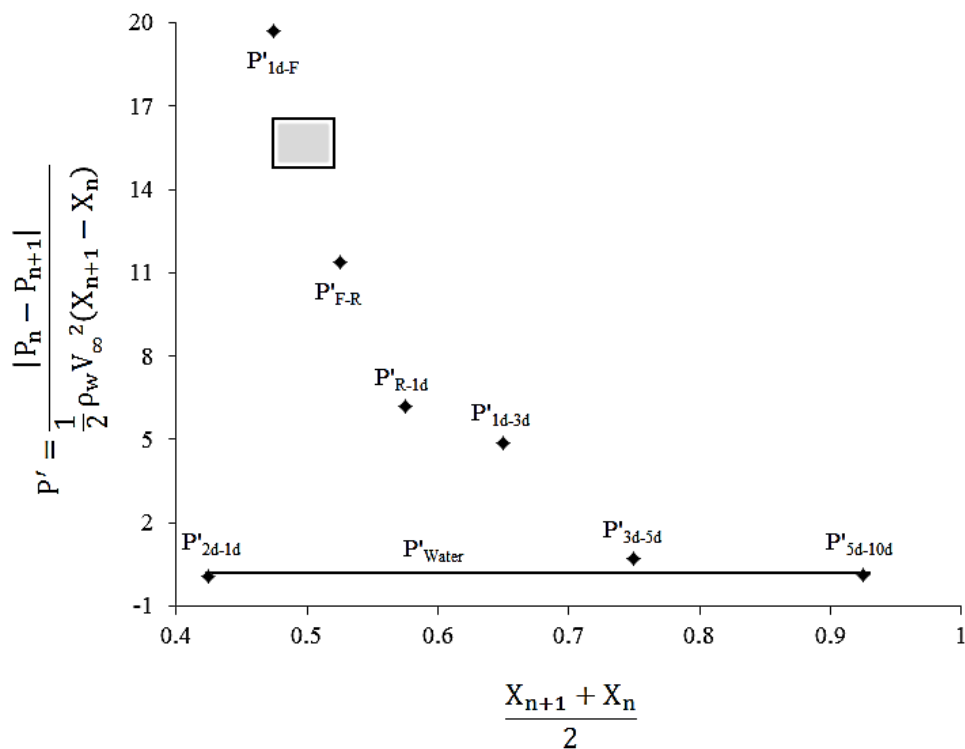


Figure 8 Variations in pressure drop across a horizontal HCP for a single equi-density cylindrical capsule of $k=0.5$ and $L_c=1d$, at $V_{av}=1\text{m/sec}$

8.1 Effect of Capsule Concentration

Figure 9 depicts the local variations in the static pressure, velocity and vorticity magnitudes within the test section of the horizontal pipe, transporting two equi-density cylindrical capsules of capsule-to-pipe diameter ratio of 0.5 at an average flow velocity of 1m/sec. The length of the capsule considered here is equal to the diameter of the capsule, whereas the spacing between the capsules is equal to one diameter of the capsule. It can be seen that the static pressure distribution around the first capsule (left) is similar to the one observed in the previous case, however, it is significantly different for the second capsule (right). This indicates that the capsule-train flow characteristics are different as compared to single-capsule flow characteristics. As compared to the previous case, when there was only one capsule present, the static pressure has slightly increased upstream of the first capsule, and is reduced further downstream. However, the static pressure variations, both upstream (-235Pa(g)) and downstream (-200Pa(g)) the second capsule, are completely different,

depicting considerably less pressure drop due to the addition of the second capsule in the pipeline. Figures 9(b) and (c) suggests that the second capsule is present in the wake of the first capsule, as the velocity profile hasn't completely developed downstream the first capsule, and the shear layers are extending farther than the second capsule's front face. Due to the presence of a second capsule, which is close-by the first capsule, the shear layers on the rear peripheral face of the first capsule gets attached to the front peripheral face of the second capsule, hence vortices are not being shed downstream the first capsule, as the shear layers of the first capsule gets energised by the shear layer of the second capsule. Furthermore, on the rear peripheral face of the second capsule, the shear layers although have no resistance downstream the capsule, however, the energy contained within the shear layers of the second capsule isn't enough to shed vortices. The consequence of this is slight reduction in the drag coefficient of the first capsule, which has been recorded to be 2.163, although the pressure drop within the pipeline is expected to be higher than the previous case of a single capsule. The drag coefficient of the second capsule is 0.125, clearly showing that second capsule's contribution towards the pressure losses within the HCP, in this particular case, is significantly less than the first capsule.

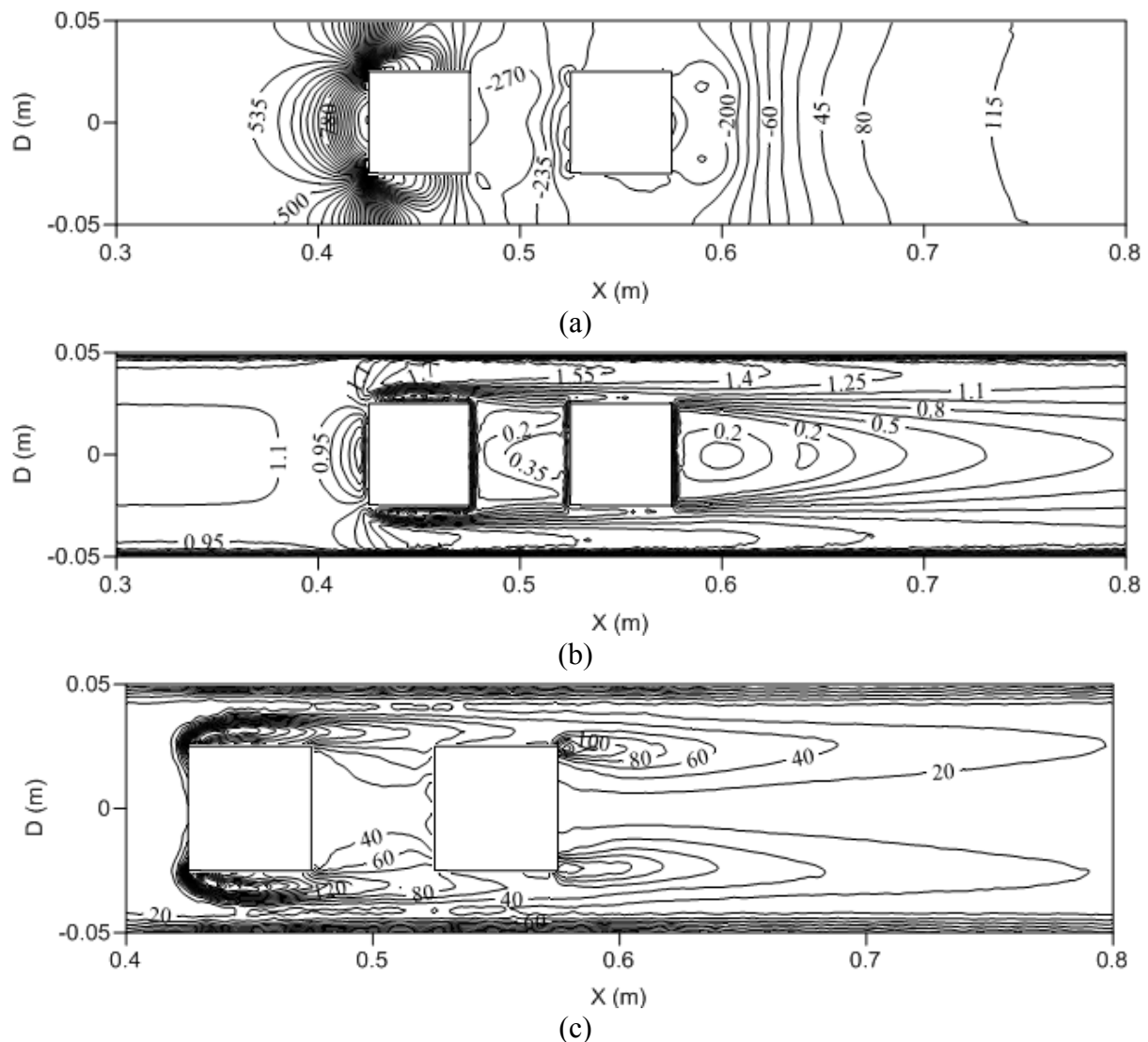


Figure 9 Flow fields within a horizontal HCP transporting two equi-density cylindrical capsules of $k=0.5$, $L_c=1d$ and $Sc=1d$ at $V_{av}=1m/sec$ (a) Static pressure (Pa) (b) Velocity magnitude (m/sec) (c) Vorticity magnitude (/sec)

The effect of the addition of a second similar cylindrical capsule, on the pressure drop across the HCP, has been depicted in figure 10. It can be seen that the introduction of the second capsule considerably affects the pressure drop variations downstream the first capsule. The first major difference with respect to the previous case can be observed between the rear face of the first capsule and 1d downstream it (i.e. $P'_{(R-1d)_1}$, 1 representing the first capsule), which is same as between the front face of the second capsule and 1d upstream it (i.e. $P'_{(1d-F)_2}$). The pressure drop between the rear face of the second capsule and location 1d downstream has increased, as evident from figure 9(a), while it keeps on decreasing thereafter until it coincides with the hydraulic pressure drop line. It is however noteworthy that the wake region of the second capsule is considerably small, as the effects of the presence of the second capsule are limited to 3d location downstream the second capsule, as compared to 5d for a single capsule.

The total pressure drop within the test section of the HCP has been calculated to be 439Pa(g), hence, f_c is 0.0695, while f_w remains the same as discussed in the previous case. The value of f_c shows that the pressure drop is higher than the previous case. It can thus be concluded that increase in the capsule concentration within an HCP increases the pressure drop within it. Moreover, two capsules that are very close-by may behave as a single long capsule within the HCP.

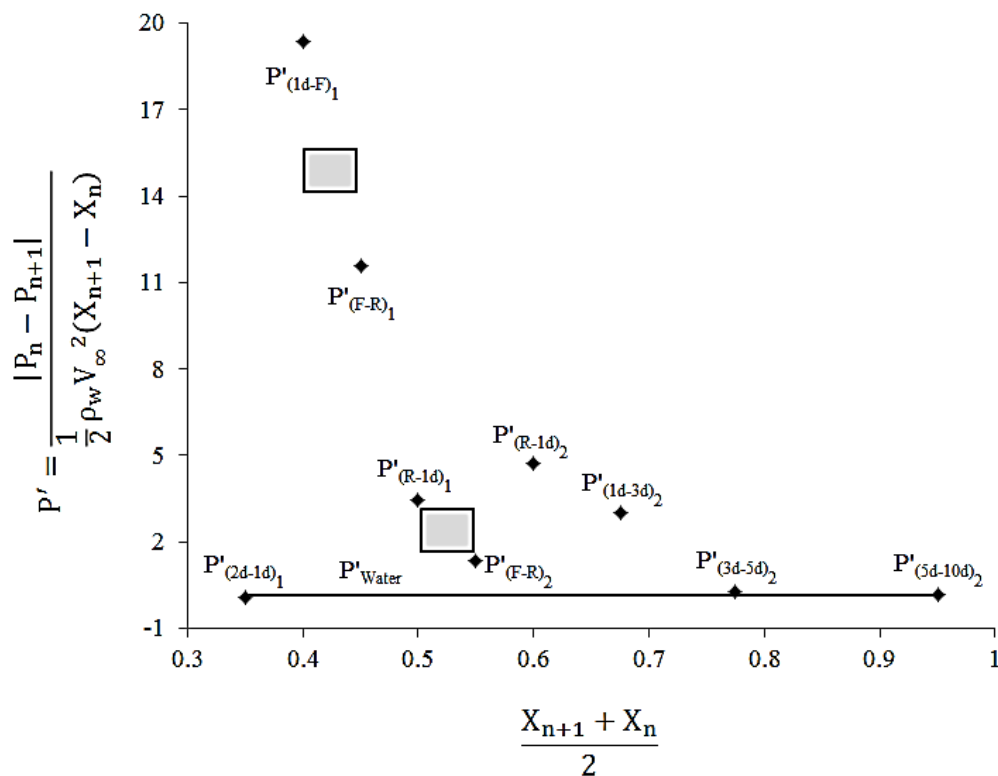


Figure 10 Variations in pressure drop across a horizontal HCP for two equi-density cylindrical capsules of $k=0.5$, $L_c=1d$ and $Sc=1d$, at $V_{av}=1m/sec$

8.2 Effect of Capsule Spacing

Figure 11 depicts the local variations in the static pressure, velocity and vorticity magnitudes within the test section of the horizontal pipe, transporting two equi-density cylindrical capsules of capsule-to-pipe diameter ratio of 0.5 at an average flow velocity of 1m/sec. The length of the capsule considered here is equal to the diameter of the capsule, whereas the spacing between the capsules is equal to five diameters of the capsule. It can be seen in figure

11(a) that the static pressure distribution around the first capsule (left) is similar to the one observed in the previous case, however, it is significantly different for the second capsule (right). This indicates that the spacing between the capsules in an HCP is an important parameter to consider while designing such pipelines. As compared to the previous case with spacing of $1d$ between the capsules, it can be seen that distinct vortices are being shed downstream the first capsule. This is because the second capsule is far-off now, and hence the shear layers of the first capsule have enough energy and space to shed vortices. However, same cannot be stated about the second capsule. Although the second capsule is far-off from the first one, it has already been discussed that a single capsule's effect can be felt upto $1d$ and $5d$ upstream and downstream the capsule. In the present case, the second capsule is $5d$ from the first capsule, whereas the second capsule's upstream effects are intersecting with first capsule's downstream effects, hence the energy contained within the shear layers of the second capsule isn't enough to shed the vortices; however, it is enough to create one, which remains attached to its shear layers via the trailing jet (as evident in figures 11(a), (b) and (c)). The drag coefficient of the first capsule is 2.153, whereas it is 1.229 for the second capsule, clearly showing that the second capsule's contribution towards the pressure losses within the HCP has significantly increased in this case. Hence, a considerably higher pressure drop across the test section of the HCP is expected.

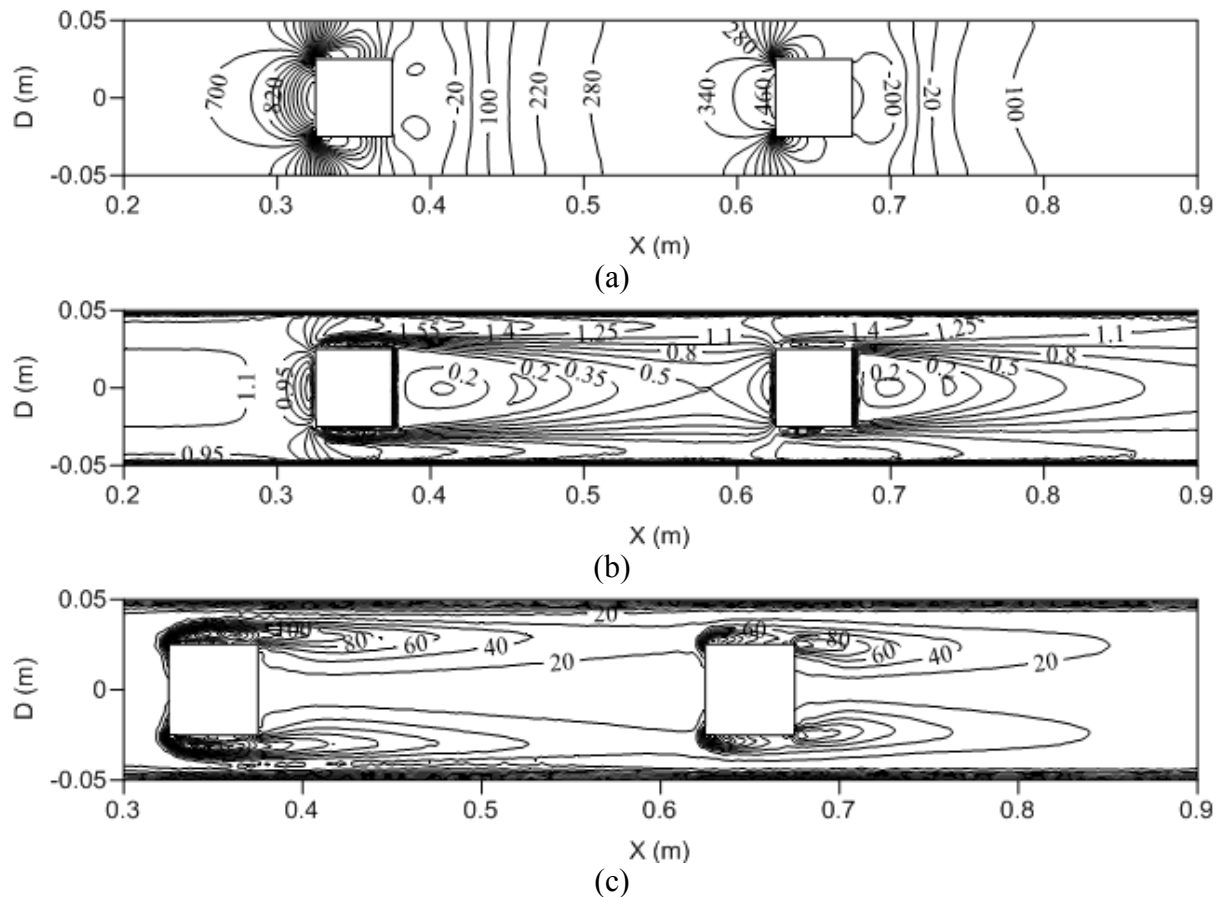


Figure 11 Flow fields within a horizontal HCP transporting two equi-density cylindrical capsules of $k=0.5$, $L_c=1d$ and $Sc=5d$ at $V_{av}=1$ m/sec (a) Static pressure (Pa) (b) Velocity magnitude (m/sec) (c) Vorticity magnitude (/sec)

The effect of increased spacing between the capsules is depicted in figure 12, which looks like the pressure drop variations of a single capsule repeated twice. The total pressure drop within the test section of the HCP has been calculated to be 603Pa(g), hence, f_c is 0.1024.

This shows that the pressure drop is considerably higher than the previous case where the spacing between the capsules was 1d. Hence, it can be concluded that increase in the spacing between the capsules increases the pressure drop within HCP upto a certain limit, after which there are is no further increase in the pressure drop across the HCP.

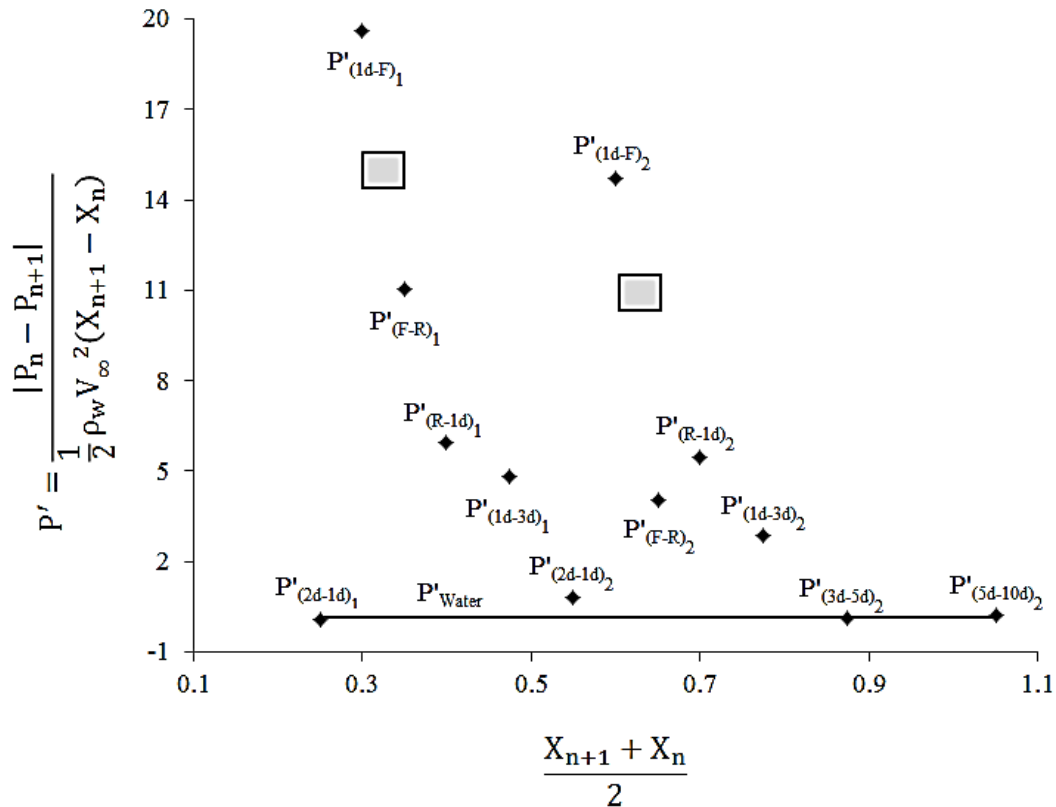


Figure 12 Variations in pressure drop across a horizontal HCP for two equi-density cylindrical capsules of $k=0.5$, $L_c=1d$ and $Sc=5d$, at $V_{av}=1m/sec$

8.3 Effect of Capsule Size

Figure 13 depicts the local variations in the static pressure, velocity and vorticity magnitudes within the test section of the horizontal pipe, transporting a single equi-density cylindrical capsule of capsule-to-pipe diameter ratio of 0.7 at an average flow velocity of 1m/sec. The length of the capsule considered here is equal to the diameter of the capsule. It can be seen in figure 13(a) that the static pressure distribution is highly non-uniform within the HCP. The static pressure difference between the upstream and downstream locations of the capsules is significantly higher than observed in case of capsule-to-pipe diameter ratio of 0.5, indicating that the pressure drop would be much higher in this case. The higher upstream static pressure is due to the larger frontal cross-sectional area of the capsule, offering more resistance to the flow of its carrier fluid within the HCP. This is further associated with the reduction in the flow velocity upstream the capsule, as depicted in figure 13(b). Same trends have been observed in case of capsule-to-pipe diameter ratio of 0.5, with the difference of the scale only, which is expected to increase drag on the capsule. The drag coefficient in this case is 4.989, which is 130% higher than for capsule-to-pipe diameter ratio of 0.5.

The flow then enters the annulus region between the pipe wall and the capsule. As the cross-sectional area decreases, the flow accelerates (as depicted in figure 13(b)), resulting in reduction in the static pressure. This is also consistent with the observations in case of capsule-to-pipe diameter ratio of 0.5; however, the cross-sectional area of the annulus is much smaller in the present case. It can be seen in figure 13(a) that although the vortices are

being formed, they remain attached to the shear layers by their trailing jets. Furthermore, it can be seen in figure 13(c) that the trends in vorticity magnitude variations are the same as observed in case of capsule-to-pipe diameter ratio of 0.5.

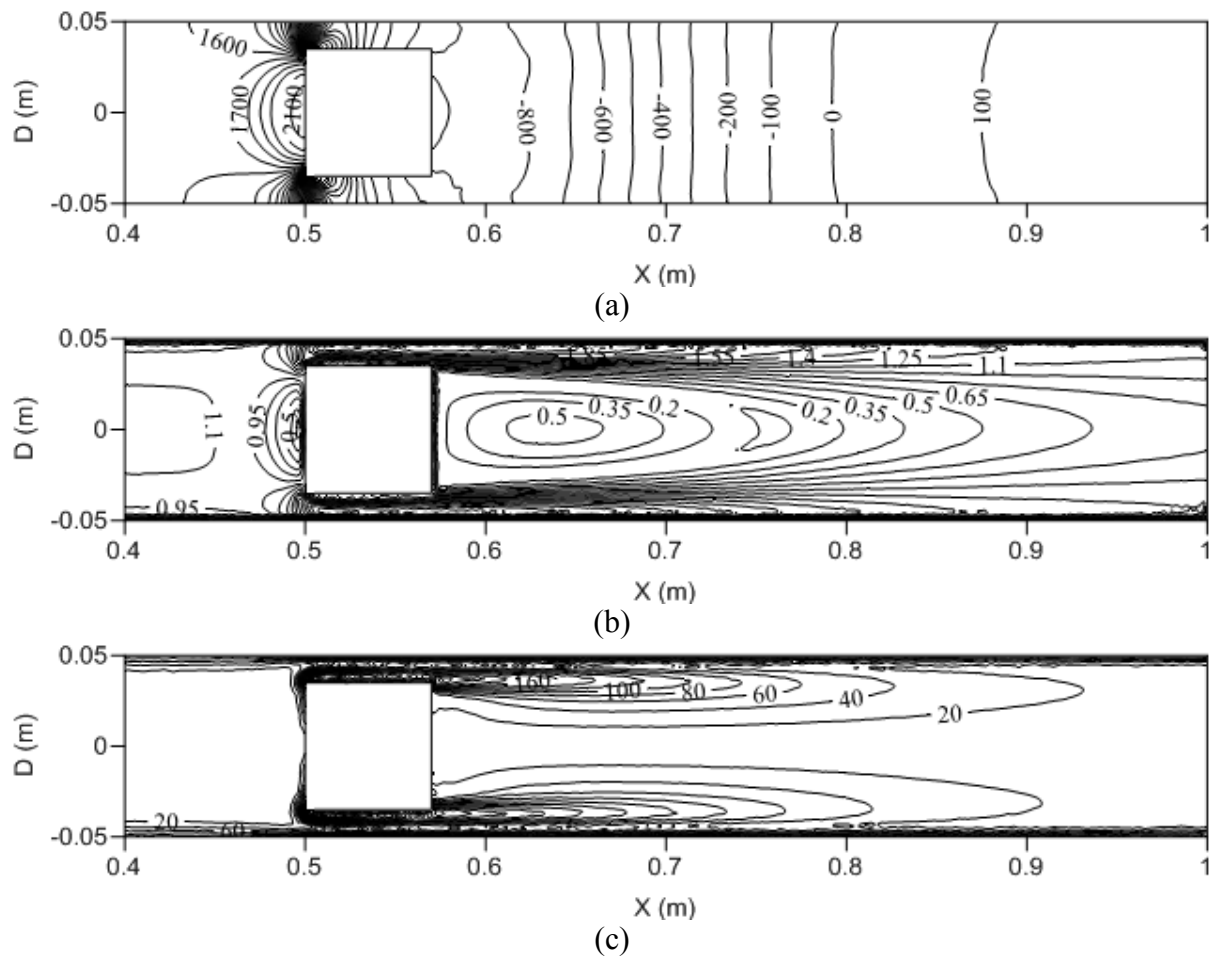


Figure 13 Flow fields within a horizontal HCP transporting a single equi-density cylindrical capsule of $k=0.7$ and $L_c=1d$ at $V_{av}=1$ m/sec (a) Static pressure (Pa) (b) Velocity magnitude (m/sec) (c) Vorticity magnitude (/sec)

The effect of increased capsule-to-pipe diameter ratio on the pressure drop across the HCP has been depicted in figure 14, which looks similar to the pressure drop variations in case of $k=0.5$, apart from the fact that the y-axis scale is much higher, indicating higher pressure drop within the HCP. Furthermore, it has been noticed that the pressure drop between the rear face of the capsule and $1d$ location downstream the capsule is less than between $1d$ and $3d$ locations downstream the capsule. This is evident from figure 13(a) that the pressure variations immediately downstream the capsule are marginal due to the presence of the attached vortices, whereas after almost $1d$ location downstream the capsule, conventional pressure variations are observed.

The value of α in the present case is 0.083, which is 82% lower than for capsule-to-pipe diameter ratio of 0.5, suggesting that the pressure drop across the test section of the HCP would be considerably higher for capsule-to-pipe diameter ratio of 0.7, as expected. The pressure drop in this particular case is 1532 Pa, which is 270% higher than for capsule-to-pipe diameter ratio of 0.5, hence the pressure drop within HCPs increases as the capsule-to-pipe diameter ratio of the capsules increases. The friction factor corresponding to the capsule

(fc) has been computed to be 0.2885, which is 347% higher than for capsule-to-pipe diameter ratio of 0.5.

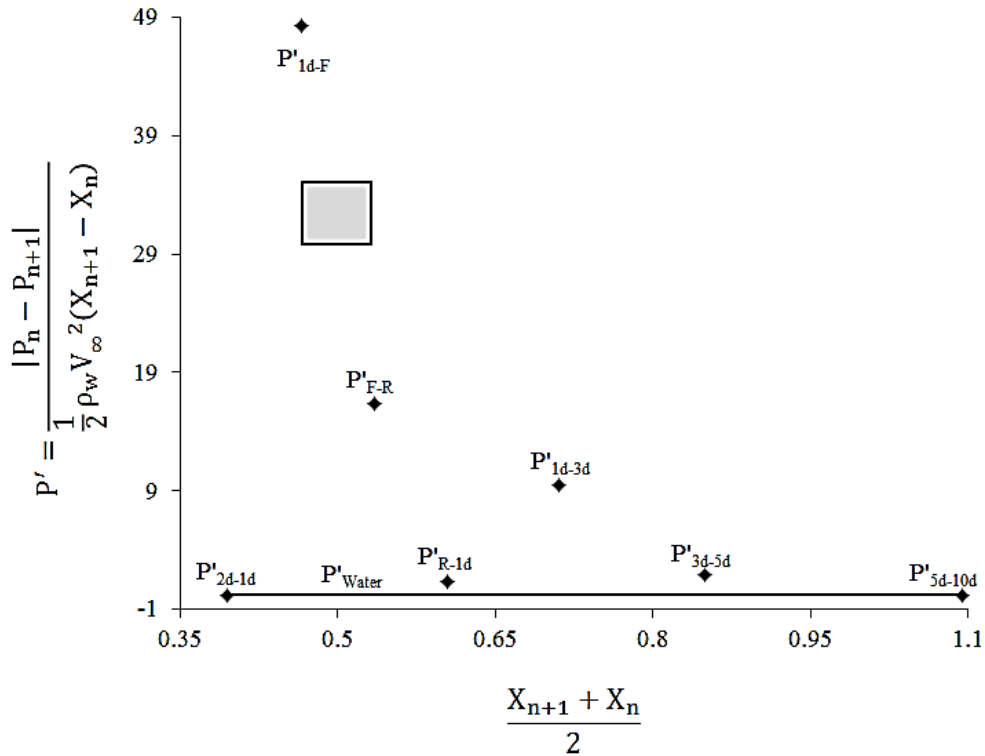


Figure 14 Variations in pressure drop across a horizontal HCP for a single equi-density cylindrical capsule of $k=0.7$ and $L_c=1d$, at $V_{av}=1m/sec$

Figure 15 depicts the local variations in the static pressure, velocity and vorticity magnitudes within the test section of the horizontal pipe, transporting a single equi-density cylindrical capsule of a longer length with capsule-to-pipe diameter ratio of 0.5 at an average flow velocity of 1m/sec. The length of the capsule considered here is equal to five times the diameter of the capsule. It can be seen in figure 15(a) that the static pressure distribution upstream the capsule is highly non-uniform and resembles that for the capsule length of 1d. Moreover, these variations can be seen in the annulus region as well, however, these effects are noticed only up to about 2d length of the capsule, after which no significant pressure variations are observed in the axial direction. Hence, the pressure drop across the test section of the HCP is expected to be in close range as that for the capsule length of 1d. The drag coefficient in this case is 2.028, as expected.

It is noteworthy that the vortices again are not being shed downstream the capsules, although they are formed by the roll-up of the shear layers. The reason behind this is the fact that although the shear layers have higher energy content near the front peripheral area of the capsule, the viscous effects gets dissipated along the axial direction, and by the time the flow exits the annulus region, the energy content of the shear layers have reduced below the threshold of vortex shedding i.e. the formation number, as discussed earlier. This is evident from figure 15(c) as well that the vorticity is being generated from the frontal periphery of the capsule, but due to longer capsule, it gets dissipated before it reaches the rear periphery of the capsule.

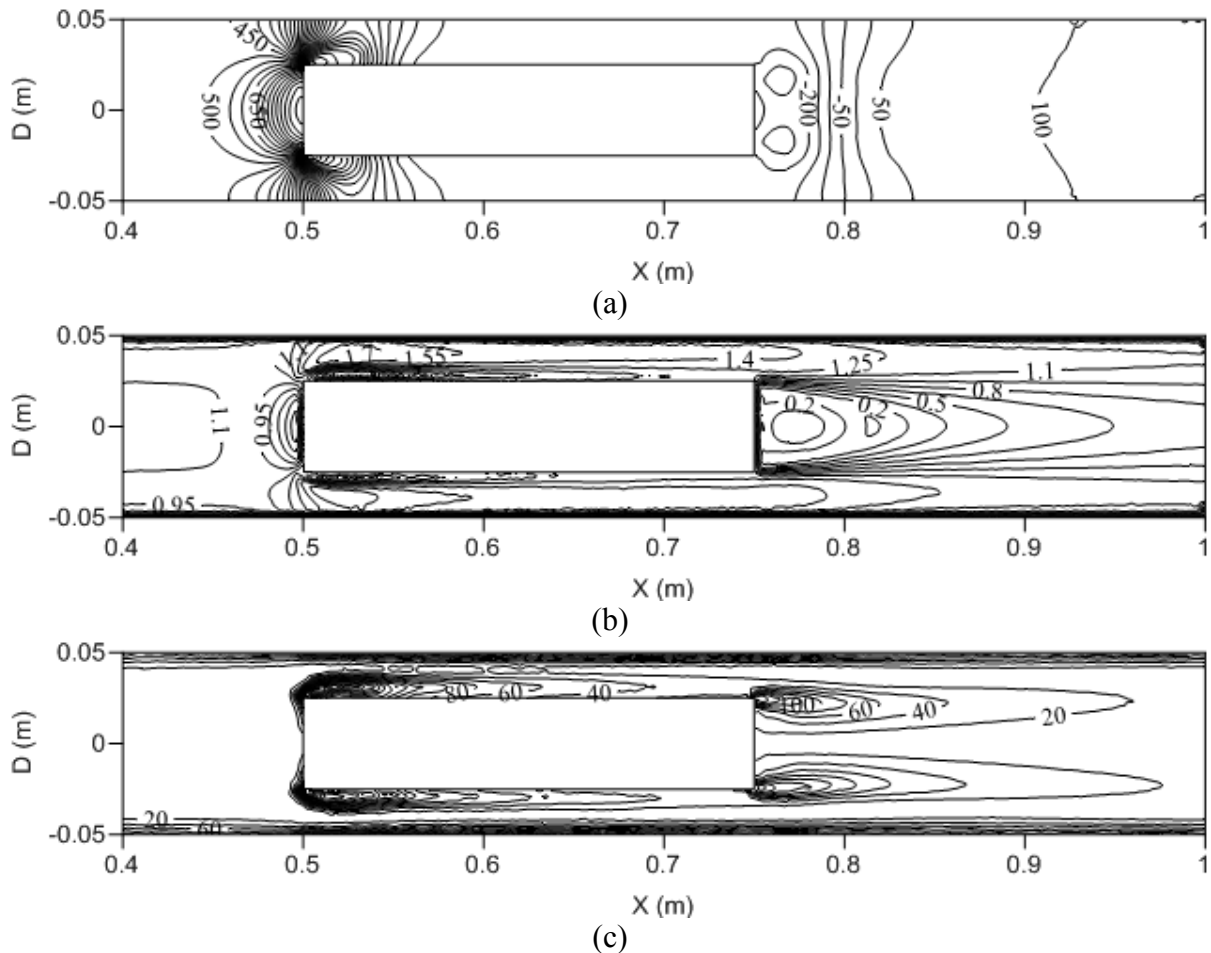


Figure 15 Flow fields within a horizontal HCP transporting a single equi-density cylindrical capsule of $k=0.5$ and $L_c=5d$ at $V_{av}=1\text{m/sec}$ (a) Static pressure (Pa) (b) Velocity magnitude (m/sec) (c) Vorticity magnitude (/sec)

The effect of increased capsule length on the pressure drop across the HCP has been depicted in figure 16, which looks similar to the pressure drop variations in case of capsule length of $1d$, apart from the fact that the y-axis scale is much smaller. This however is not indicative of lower pressure drop across the test section of the HCP because $1d$ axial length in the present case corresponds to 0.25m , whereas it was 0.05m in case of capsule length of $1d$. Hence, figure 16 provides qualitative information primarily, rather than quantitative information about the pressure drop across the HCP. In order to get a realistic prediction of pressure drop across the test section of the HCP, α can be used in the present case, which is computed to be 0.466 . The value of α in case of capsule length of $1d$ was also 0.466 , indicating that the pressure drop across the HCP remains almost the same for longer capsules within this range, which is a very important information as far as cargo transport through capsules is concerned. Pressure drop across the test section of the HCP has been calculated to be 415Pa(g) , whereas it was 414Pa(g) for the capsule of length of $1d$. Hence, the length of the capsule, within the range considered in the present study, has negligibly small effect of the pressure drop within HCPs. This means that more cargo can be transported with longer capsules at relatively minor extra cost. The friction factor corresponding to the capsule (f_c) in the present case is 0.0647 .

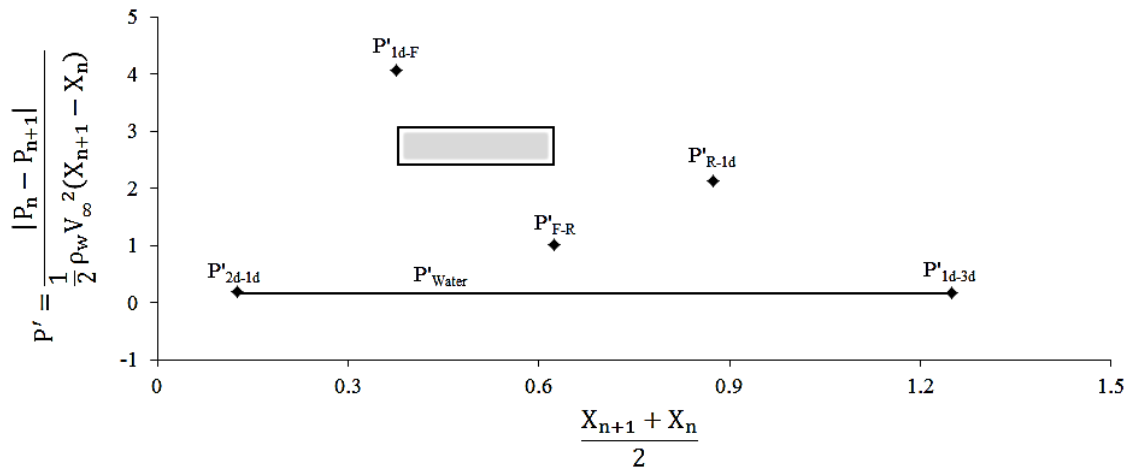
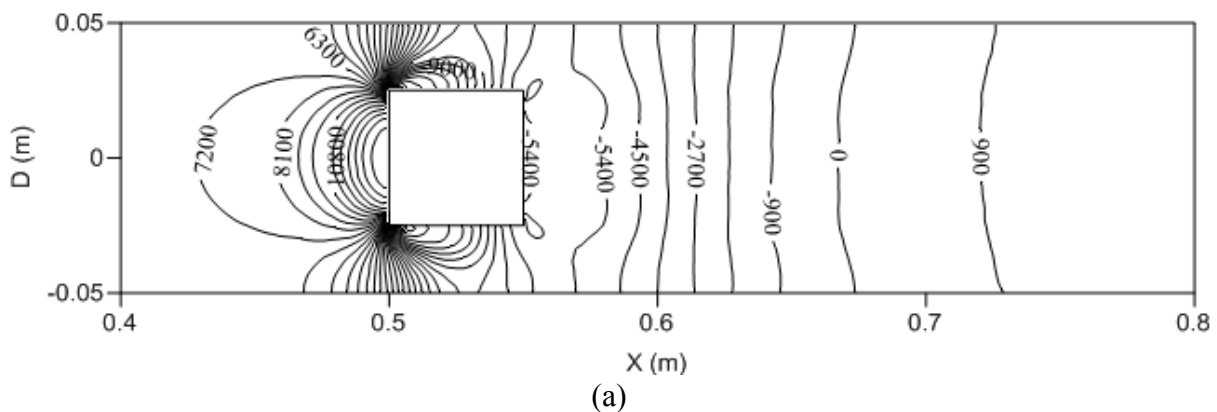


Figure 16 Variations in pressure drop across a horizontal HCP for a single equi-density cylindrical capsule of $k=0.5$ and $Lc=5d$, at $V_{av}=1\text{m/sec}$

8.4 Effect of Flow Velocity

Figure 17 depicts the local variations in the static pressure, velocity and vorticity magnitudes within the test section of the horizontal pipe, transporting a single equi-density cylindrical capsule of capsule-to-pipe diameter ratio of 0.5 at an average flow velocity of 4m/sec. The length of the capsule considered here is equal to the diameter of the capsule. It can be seen in figure 17(a) that the static pressure distribution is highly non-uniform within the HCP. The static pressure difference between the upstream and downstream locations of the capsules is significantly higher than observed in case of capsule flow with average water flow velocity of 1m/sec, as expected from equation (5), indicating that the pressure drop would be significantly higher. The pressure variations observed here are consistent with the trends observed in case of average flow velocity of 1m/sec, with the difference of the scale only, however, the non-dimensional pressure drag coefficient is not expected to increase because of the same frontal area of the capsule. The drag coefficient in this case is 2.202, which is almost the same as for average flow velocity of 1m/sec. Furthermore, figures 17(b) and (c) depicts higher flow velocities and higher vorticity magnitude within the test section of the HCP, which is again due to higher average flow velocity, and hence non-dimensional analysis becomes ever more important in this case.



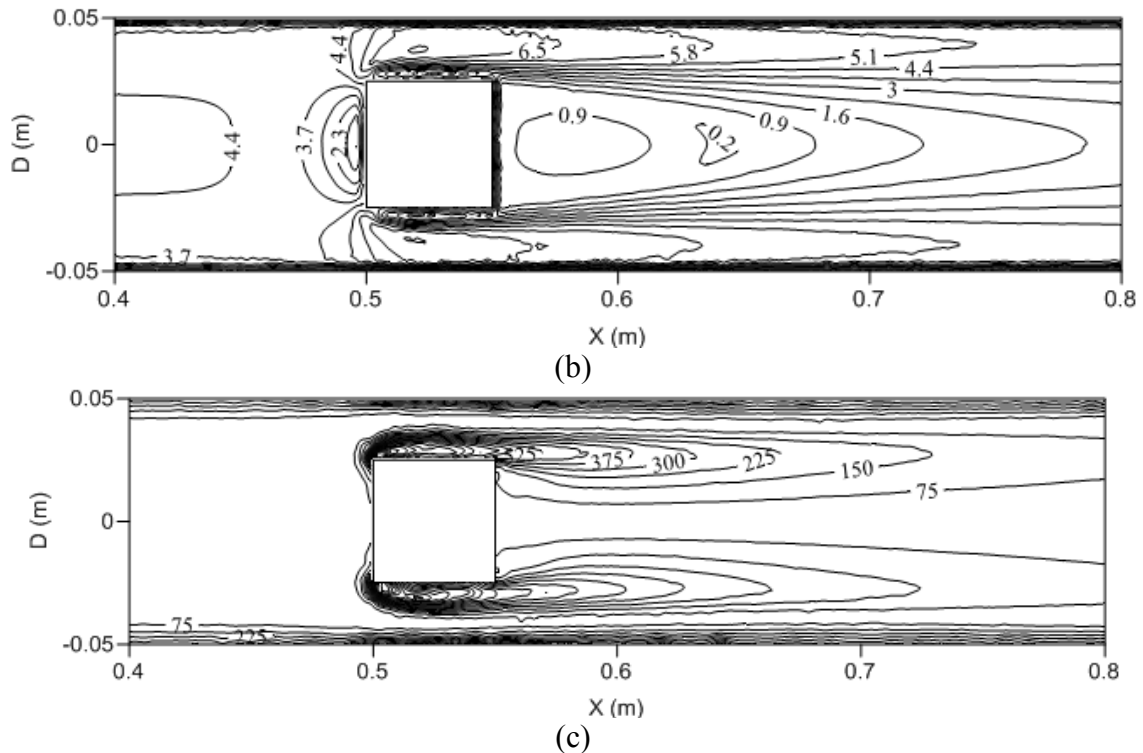


Figure 17 Flow fields within a horizontal HCP transporting a single equi-density cylindrical capsule of $k=0.5$ and $L_c=1d$ at $V_{av}=4m/sec$ (a) Static pressure (Pa) (b) Velocity magnitude (m/sec) (c) Vorticity magnitude (/sec)

The effect of increased average flow velocity on the pressure drop across the HCP has been depicted in figure 18, which remains the same as compared to $V_{av}=1m/sec$, both in trends and magnitude. Hence, the non-dimensional pressure drop is independent of the average flow velocity within an HCP. This is of particular importance to HCP designers while choosing an appropriate pumping power, and the distance between consecutive pumping stations. The value of α in the present case is 0.047, which is the same as for average flow velocity of 1m/sec, further indicating that average flow velocity has no effect on non-dimensional pressure drop within an HCP. This means that although the pressure drop across the pipeline would be higher at higher flow velocities, the pressure distribution remains the same in the pipeline. The pressure drop in this case is 6208Pa(g), which is 14 times higher than at an average flow velocity of 1m/sec. The friction factors f_w and f_c have been computed to be 0.0138 and 0.0639 respectively. A lower f_w was expected, as it is an established fact that as Reynolds number of a single phase flow increases, f_w decreases [45].

8.5 Effect of Capsule Density

Figure 19 depicts the local variations in the static pressure, velocity and vorticity magnitudes within the test section of the horizontal pipe, transporting a single heavy-density cylindrical capsule of capsule-to-pipe diameter ratio of 0.5 at an average flow velocity of 1m/sec. The length of the capsule considered here is equal to the diameter of the capsule. It can be seen in figure 17(a) that because the capsule is heavier than its carrier fluid; it propagates along the bottom wall of the pipe. The static pressure distribution is highly non-uniform within the HCP with areas of recirculation both upstream and downstream the capsule. Furthermore, it can be seen that the effect of the capsule is felt much farther downstream the capsule. This deviation in the flow field is expected to generate more secondary flows, as can be observed in figure 19(c), hence, increasing the pressure drop within the test section of the HCP to some extent.

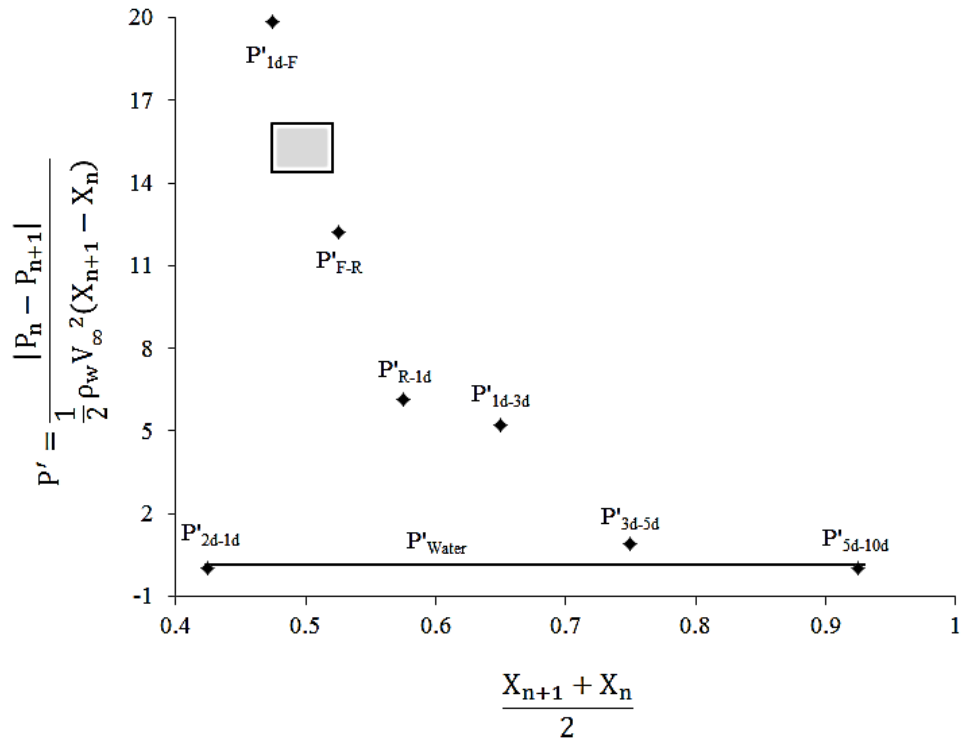
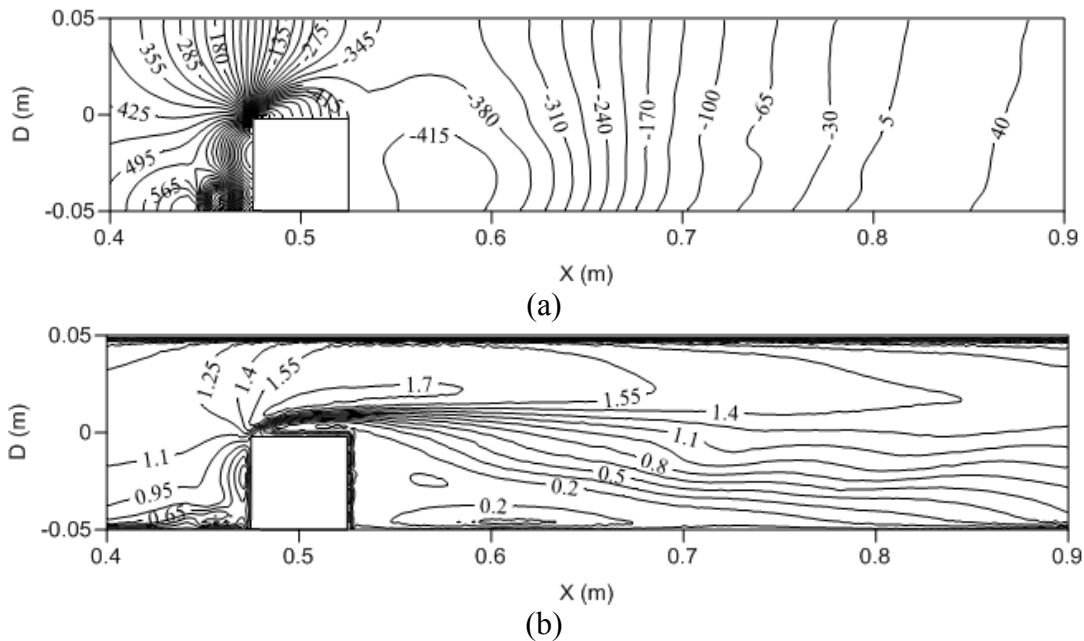


Figure 18 Variations in pressure drop across a horizontal HCP for a single equi-density cylindrical capsule of $k=0.5$ and $Lc=1d$, at $V_{av}=4m/sec$

The value of α has been calculated to be 0.35 in the present case, which is 24.8% less than for an equi-density cylindrical capsule, indicating higher pressure drop within the pipeline. Moreover, the drag coefficient has been computed to be 2.155, which is almost the same as in case of an equi-density cylindrical capsule. Even though the drag coefficient of the capsule has decreased marginally (0.64%), the pressure drop is slightly higher in the pipeline because of the secondary flows downstream the capsule, which disrupts the flow, hence extracting energy from it.



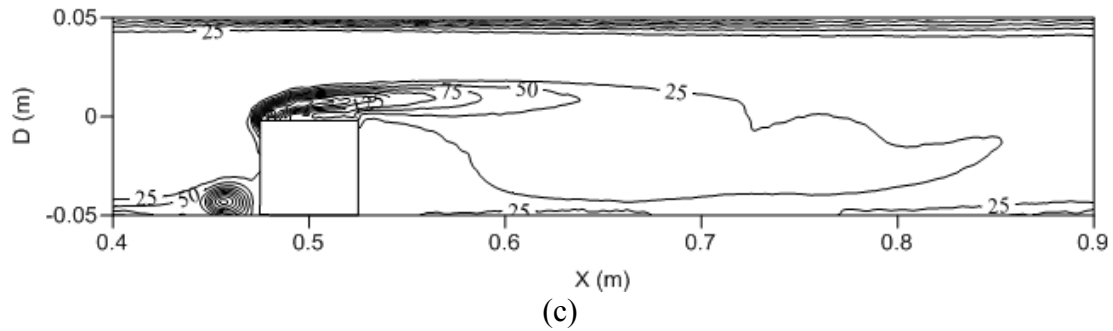


Figure 19 Flow fields within a horizontal HCP transporting a single heavy-density cylindrical capsule of $k=0.5$ and $Lc=1d$ at $V_{av}=1\text{m/sec}$ (a) Static pressure (Pa) (b) Velocity magnitude (m/sec) (c) Vorticity magnitude (/sec)

The effect of increased density of the capsule on the pressure drop across the HCP has been depicted in figure 20, which remains the same as compared to an equi-density capsule, both in trends and magnitude. Hence, the non-dimensional pressure drop is marginally dependent on the density of the capsule within an HCP. This is of particular importance to HCP designers while choosing an appropriate pumping power for a particular cargo. The pressure drop across the test section of the HCP has been computed to be 4308Pa(g) , which is 3.8% higher than for an equi-density capsule. It can thus be concluded that as the density of a capsule increases, the pressure drop within the HCP increases slightly. The friction factor for capsules (f_c) has been computed to be 0.0677, which is 4.9% higher than for an equi-density cylindrical capsule, indicating the capsule is contributing more towards the pressure drop within the HCP. f_c has later been used to develop semi-empirical novel expressions to accommodate the effects of capsule density/specific gravity on the pressure drop, for designing HCPs.

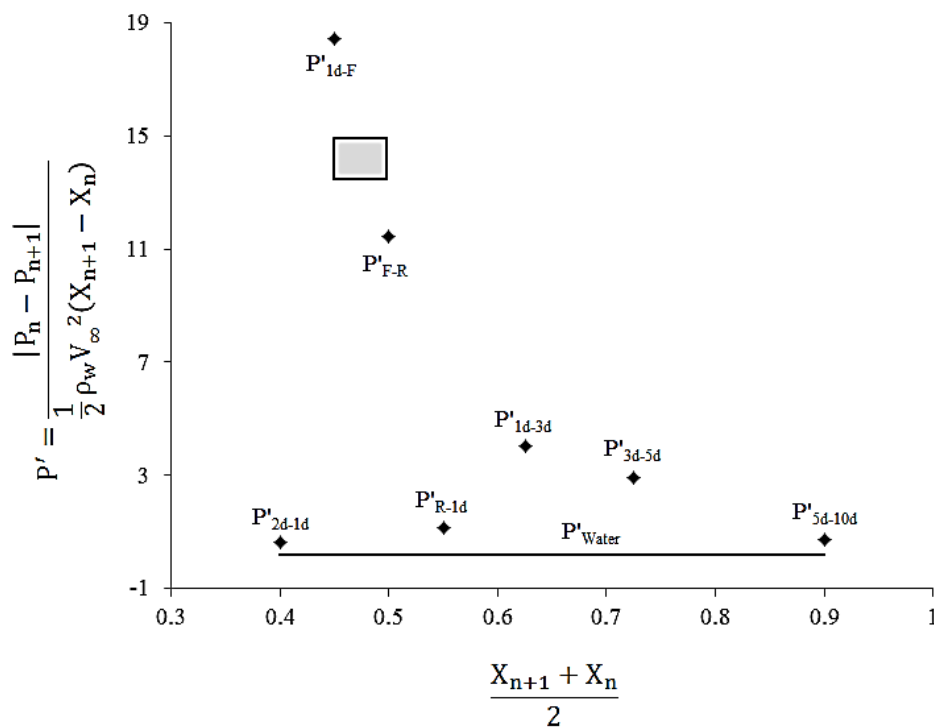


Figure 20 Variations in pressure drop across a horizontal HCP for a single heavy-density cylindrical capsule of $k=0.5$ and $Lc=1d$, at $V_{av}=1\text{m/sec}$

8.6 Effect of Pipe's Inclination

Pipelines mostly used in off-shore installations comprise of vertical pipes and pipe fittings. In order to cover a wide range of applications for HCPs, vertical HCP pipes have also been considered in the present investigation. Figure 21 depicts the local variations in the static pressure, velocity and vorticity magnitudes within the test section of the vertical pipe, transporting a single equi-density cylindrical capsule of capsule-to-pipe diameter ratio of 0.5 at an average flow velocity of 1m/sec. The length of the capsule considered here is equal to the diameter of the capsule. It can be seen that the flow fields in a vertical HCP resembles that of a horizontal HCP for the flow of equi-density cylindrical capsules. While heavy-density cylindrical capsules slides along the bottom wall of a horizontal HCP, they travel along the central axis of the vertical HCP. Hence, the flow of heavy-density cylindrical capsules in vertical HCPs also resembles the flow of equi-density cylindrical capsules in both horizontal and vertical HCPs.

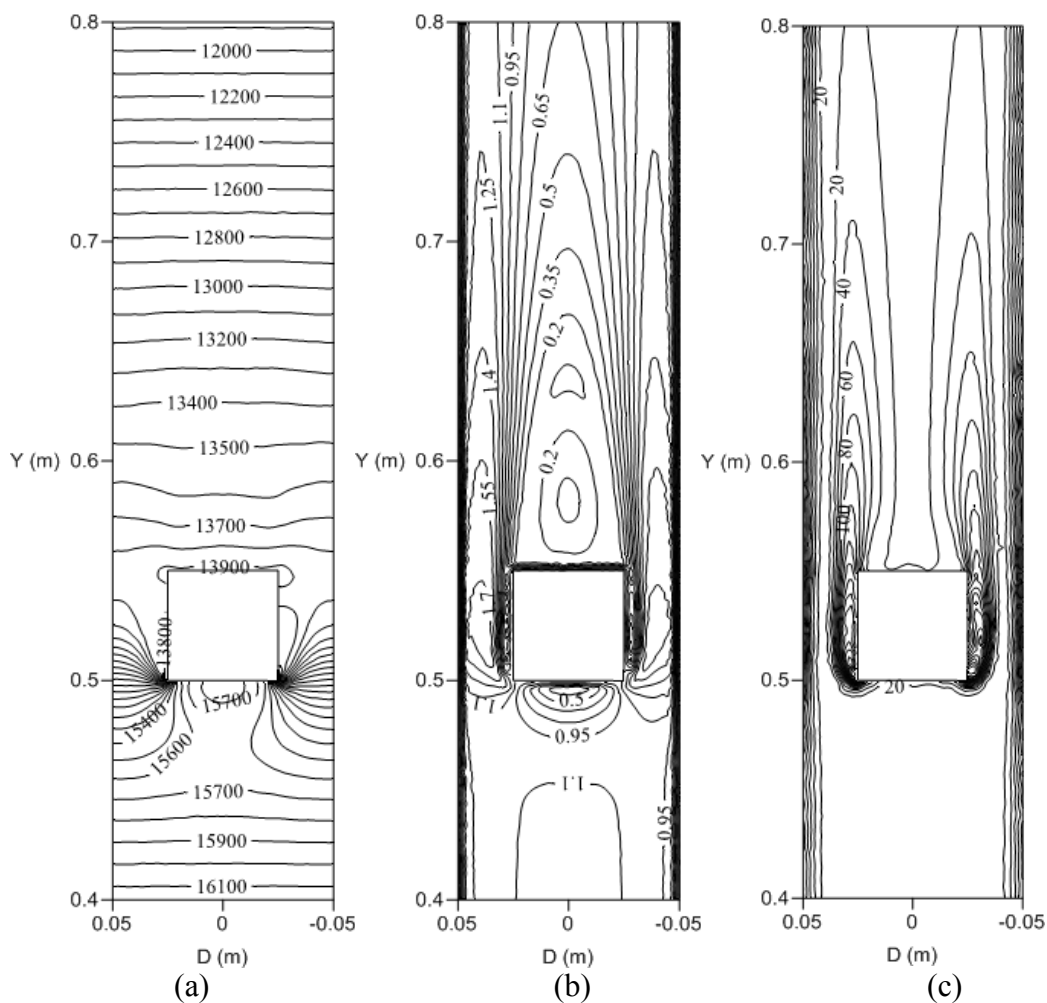


Figure 21 Flow fields within a vertical HCP transporting a single equi-density cylindrical capsule of $k=0.5$ and $L_c=1d$ at $V_{av}=1\text{m/sec}$ (a) Static pressure (Pa) (b) Velocity magnitude (m/sec) (c) Vorticity magnitude (/sec)

From equation (6), it is expected that due to the elevation of the pipeline there will be additional pressured drop as compared to a horizontal pipeline in addition to pressure drop caused because of difference in local flow features between the two. The same has been observed in case of a vertical HCP, where the pressure drop across the test section of the vertical HCP is significantly higher than for a horizontal HCP. After carrying out detailed

quantitative analysis, it has been found out that the higher pressure drop within a vertical HCP is due to the elevation of the pipeline only, and the contribution of the capsule towards the pressure drop across a vertical HCP is the same as in case of a horizontal HCP. This is further summarised in table 6 which shows the pressure drop contribution in the two pipelines (horizontal and vertical) by the capsule only. Hence, it can be concluded that equi-density cylindrical capsules, either in a horizontal or vertical pipelines, contributes the same pressure drop; however, the same cannot be stated about the heavy-density cylindrical capsules, as the flow behaviour in the two pipelines would be altogether different.

Table 6 Pressure drop comparison, due to a single equi-density cylindrical capsule only, in Horizontal and Vertical HCPs

k	Vav	ΔP_c (Horizontal Pipe)	ΔP_c (Vertical Pipe)
0.5	1	322	333
0.5	2	1283	1296
0.5	3	2876	2893
0.5	4	5104	5122
0.7	1	1440	1449
0.7	2	5673	5689
0.7	3	12696	12712
0.7	4	22471	22489

The value of α in a vertical HCP has been computed to be -0.731 because the static pressure acting on the front face of the capsule is lower than at the freestream location, as can be observed in figure 21(a). The drag coefficient of the capsule is 3.17, which is 46% higher than in a horizontal HCP. Furthermore, the non-dimensional pressure drop across the vertical HCP has been depicted in figure 22. It can be seen in the figure that the pressure drop increases significantly between the front face and 1d upstream location of the capsule, which then drops across the capsule. The pressure drop between the rear face and 1d location downstream the capsule further reduces below the water pressure drop line. This means that the static pressure is higher on the rear face of the capsule as compared to when no capsules are present in the vertical pipe. Looking closely downstream the capsule in figure 21(a), it can be seen that the static pressure difference between the rear end of the capsule (i.e. at $y=0.55m$) and 1d downstream the capsule (i.e. $y=0.6m$) is 250Pa(g), whereas in case of water flow only, the pressure drop in a vertical pipe between the same locations is 489Pa(g). Hence, the pressure drop immediately downstream the capsule is less than for water flow alone. The pressure drop increases between 1d and 5d locations downstream the capsule, until it becomes equal to the water pressure drop. Capsule friction factor (f_c) has computed to be 0.0667 in this case, which is marginally higher than in a horizontal HCP.

8.7 Capsule Flow in Bends

Minor losses in the pipeline cannot be looked over while designing a pipeline, which is true for HCPs as well. Hence, a detailed investigation on HCP bends has been included in the present study, which is of utmost importance to the pipeline designers as the availability of this information is very limited in the literature. Figure 23 depicts the local variations in the static pressure, velocity and vorticity magnitudes within a horizontal HCP bend of bend-to-pipe radius ratio of 4 carrying a single equi-density cylindrical capsule of capsule-to-pipe diameter ratio of 0.5 at an average flow velocity of 1m/sec. The length of the capsule considered here is equal to the diameter of the capsule. It can be seen in figure 23(a) that the pressure distribution within an HCP bend is altogether different to the one observed in case of a straight HCP, due to the curvature of the pipeline. Although the pressure distribution is

somewhat similar upstream the capsule, it is very different downstream it. The secondary flow generating capability within an HCP is considerably more; with many recirculating zones present downstream the capsule.

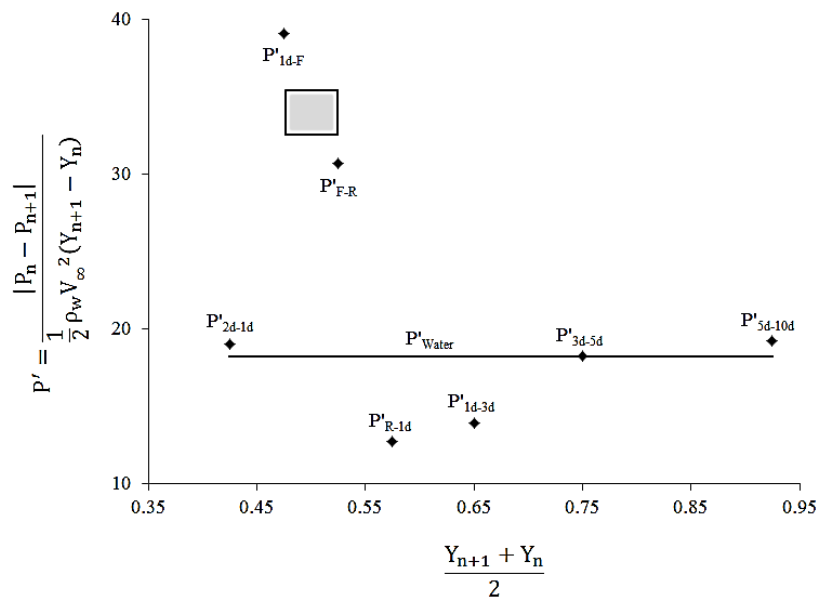
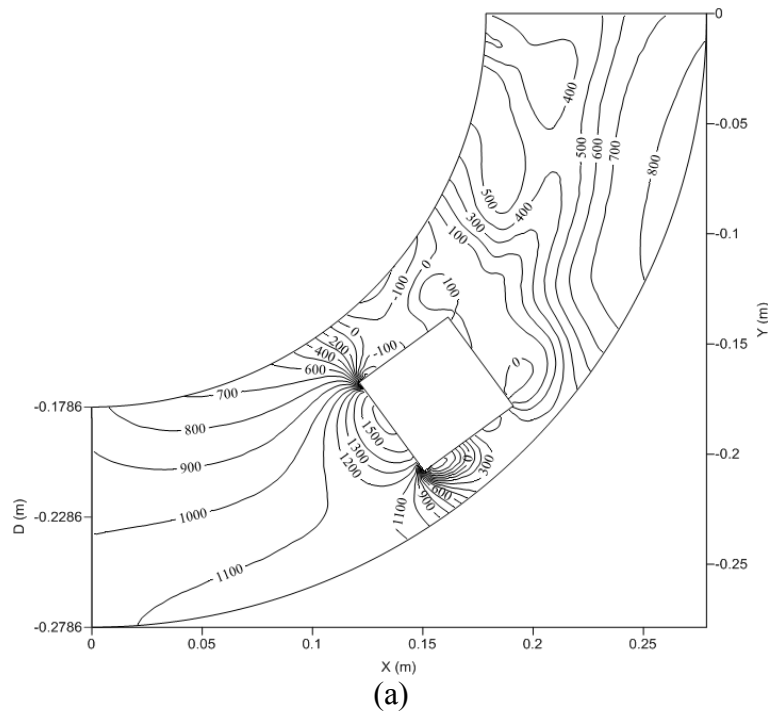
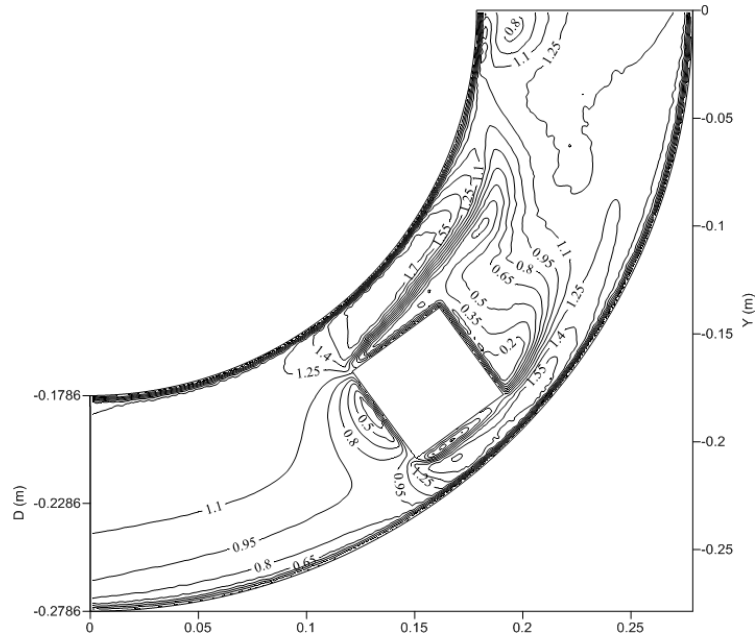


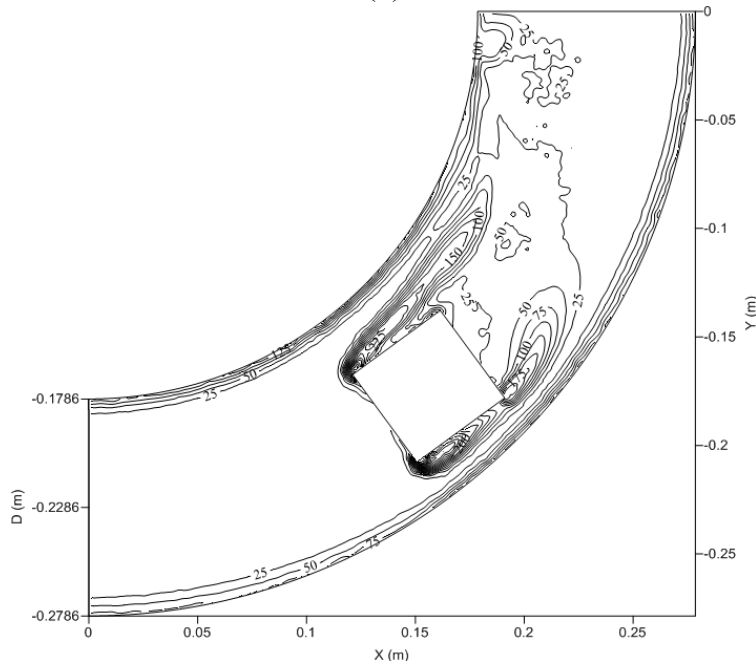
Figure 22 Variations in pressure drop across a vertical HCP for a single equi-density cylindrical capsule of $k=0.5$ and $Lc=1d$, at $V_{av}=1m/sec$

The velocity profiles (figure 23 (b)) downstream the capsule have been observed to be varying till the end of the bend, and similar trends are noticed in case of vorticity magnitude distribution as well (figure 23 (c)). Because the capsule, at this particular location and orientation within the HCP bend, is nearer to the bottom wall of the bend, uneven vortices are being shed from either ends of the capsule, downstream it.





(b)



(c)

Figure 23 Flow fields within a horizontal 90° HCP bend of $R/r=4$, transporting a single equi-density cylindrical capsule of $k=0.5$ and $Lc=1d$ at $V_{av}=1\text{m/sec}$ (a) Static pressure (Pa) (b) Velocity magnitude (m/sec) (c) Vorticity magnitude (/sec)

The value of α in the present case has found out to be 0.389, which is 16.4% less than in a horizontal pipe, indicating higher pressure drop within an HCP bend. Furthermore, the drag coefficient has been computed to be 2.419, which are 11.5% higher as compared to a horizontal HCP. Moreover, a pressure drop comparison for the present case, with horizontal straight pipe and similar bend with water flow only, has been presented in figure 24. The x-axis of the figure is computed in such a way as the capsule was present in a straight horizontal pipe, for effective comparison purposes. Both the hydraulic pipe and hydraulic bend pressure drop curves have also been plotted, which appear to coincide; however, the

non-dimensional pressure drop value in a hydraulic pipe is 0.1722, while that in case of a hydraulic bend is 0.2. Hence, the pressure drop increases in a hydraulic bend, as compared to a straight pipe, which is an established fact [46].

It can be seen in the figure that the pressure drop variations within a horizontal HCP bend resembles the one observed in case of a horizontal pipe, with the main difference in the scale of the pressure drop values. The pressure drop increase upstream the capsule up to its front end, and then it constantly decreases until it coincides with the P'_{Bend} line. It can be further noticed that due to higher curvature of the bend in the present case, the secondary flows are dissipated rapidly downstream the capsule, and hence, the effect of the capsule is felt only till 3d location downstream the capsule. K_{lc} has been computed to be 0.07413 in the present case, which is 13% higher than the friction factor f_c for the flow of an equi-density cylindrical capsule in a horizontal HCP. K_{lc} has later been used to develop semi-empirical novel expressions to accommodate the minor losses within HCPs, for design purposes.

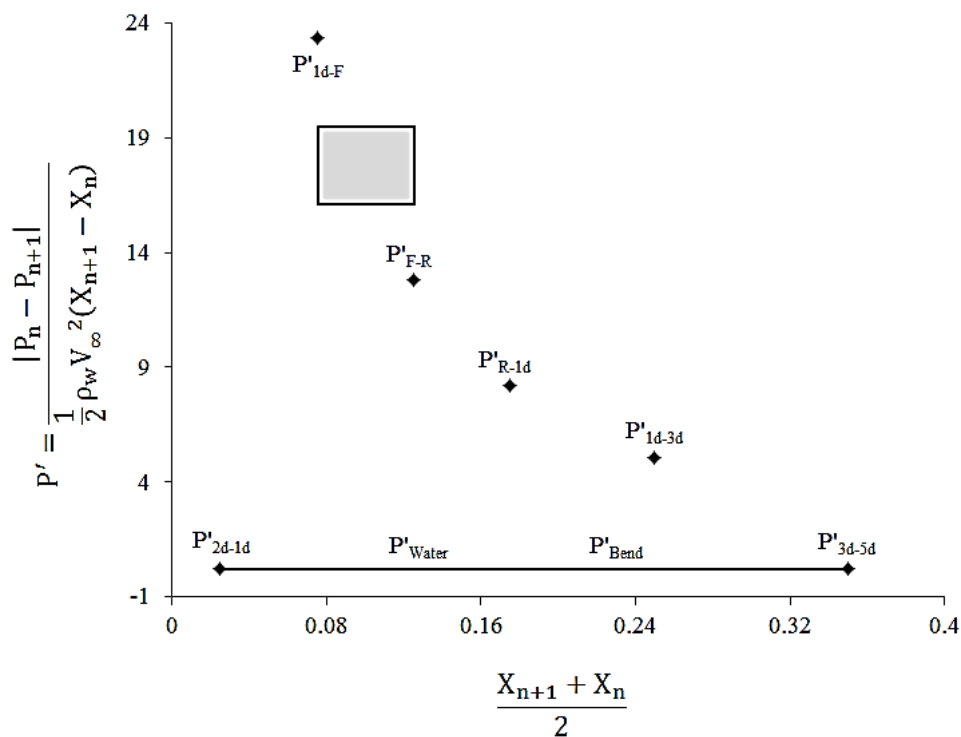
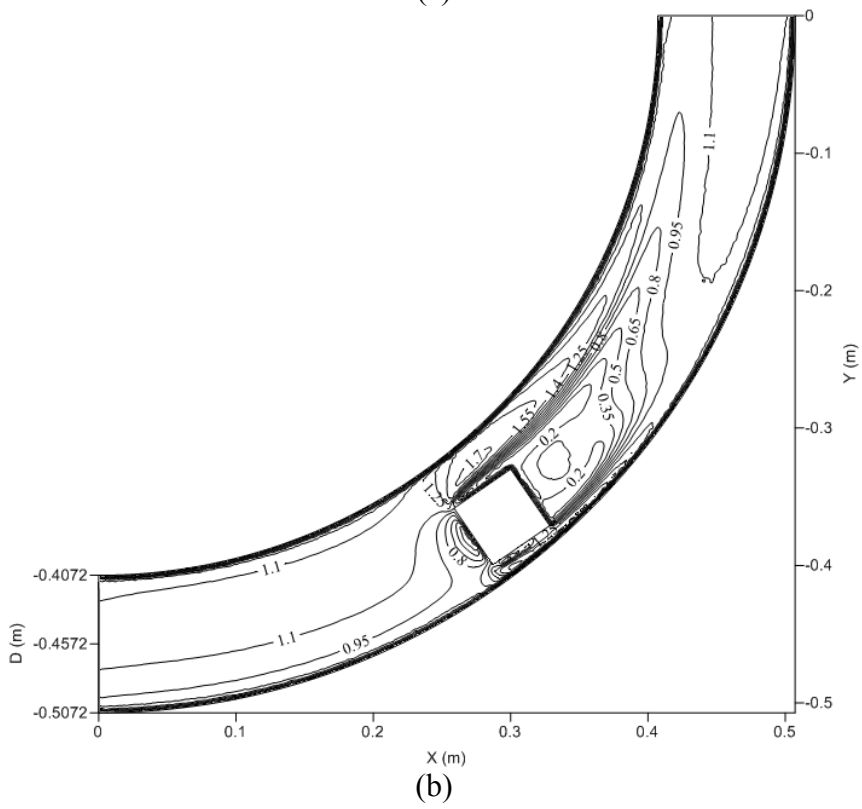
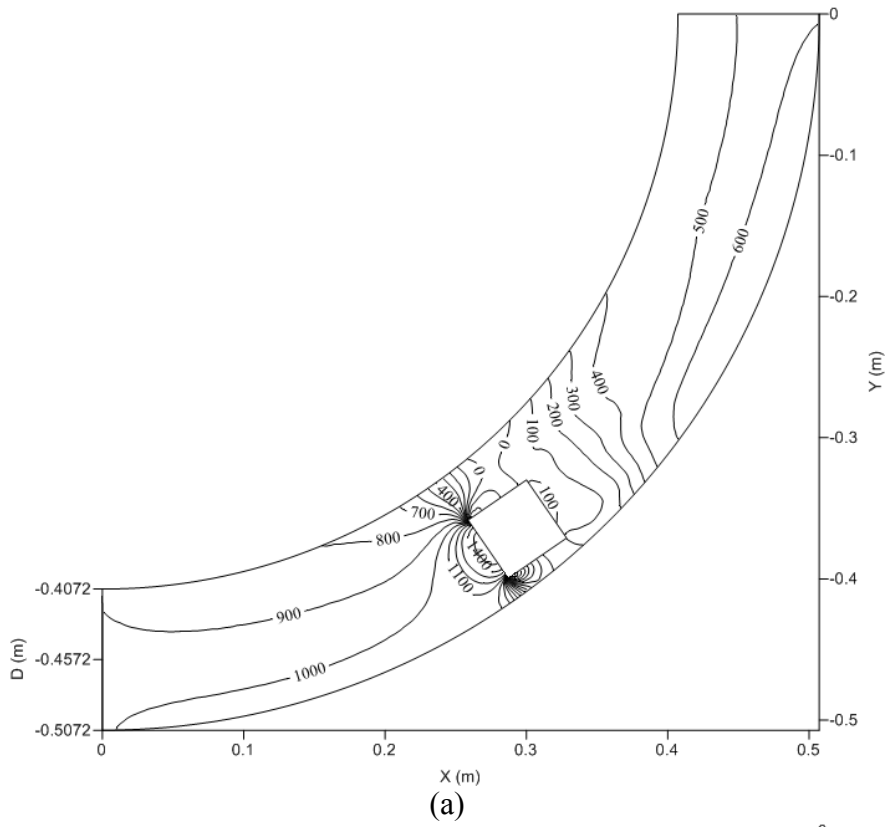


Figure 24 Variations in pressure drop across a horizontal HCP bend of $R/r=4$, for a single equi-density cylindrical capsule of $k=0.5$ and $L_c=1d$, at $V_{av}=1\text{m/sec}$

8.8 Effect of Curvature of the Bend

Figure 25 depicts the local variations in the static pressure, velocity and vorticity magnitudes within a horizontal HCP bend of bend-to-pipe radius ratio of 8 carrying a single equi-density cylindrical capsule of capsule-to-pipe diameter ratio of 0.5 at an average flow velocity of 1m/sec. The length of the capsule considered here is equal to the diameter of the capsule. It can be seen in figure 25(a) that the pressure distribution is somewhat similar to the one observed in the previous case; however, the variations in the static pressure downstream the capsule are more subtle. This is because the radius of curvature of the bend in the present case is more; hence it resembles more to a straight pipe, as compared to the previous case. This implies that the secondary flow generating capability within this bend is considerably less, with no distinct recirculating zone observed downstream the capsule. The velocity profiles downstream the capsule have been observed to be varying till the end of the bend, while vorticity profiles are contained within a finite distance downstream the capsule.



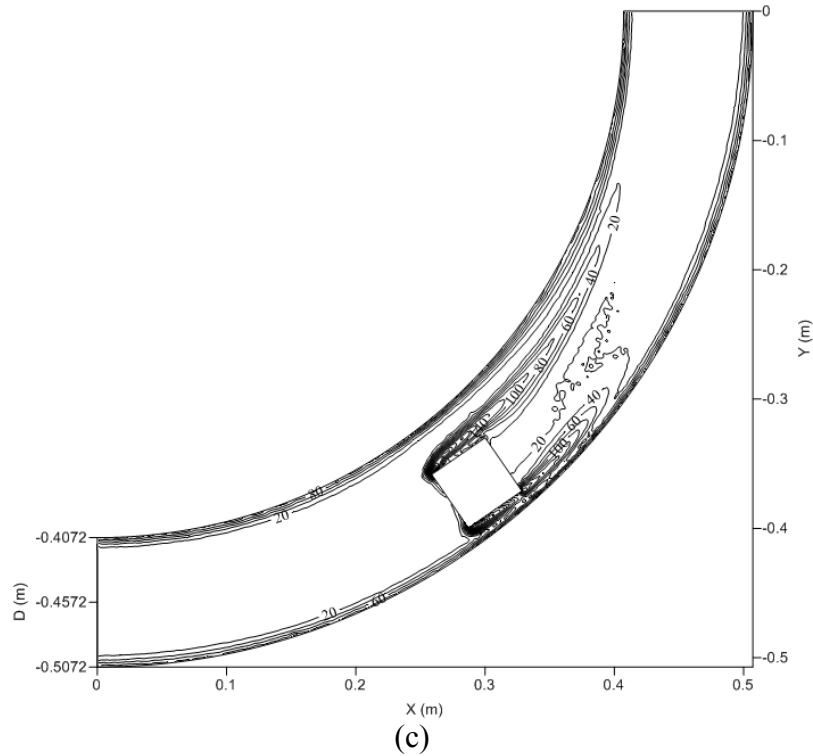


Figure 25 Flow fields within a horizontal 90° HCP bend of $R/r=8$, transporting a single equi-density cylindrical capsule of $k=0.5$ and $Lc=1d$ at $V_{av}=1\text{m/sec}$ (a) Static pressure (Pa) (b) Velocity magnitude (m/sec) (c) Vorticity magnitude (/sec)

The value α in the present case has found out to be 0.463, which is higher than the previous case of bend-to-pipe radius ratio of 4, indicating lower pressure drop as bend-to-pipe radius ratio increases. This is because of the more uniform flow and reduced secondary flows within the bend. Furthermore, the drag coefficient has been computed to be 2.297, which is 5% less than for bend-to-pipe radius ratio of 4, indicating lower pressure drop within this bend. The reduction in drag coefficients is because there is less resistance to the flow (because of directional change) within the bend of bend-to-pipe radius ratio of 8, hence this bend is straighter than the bend with bend-to-pipe radius ratio of 4. Moreover, a pressure drop comparison for the present case, with horizontal straight pipe and similar bend with water flow only, has been presented in figure 26. The non-dimensional pressure drop value in a hydraulic pipe is 0.1722, while that in case of a hydraulic bend is 0.188, which is lower than in case of bend with bend-to-pipe radius ratio of 4. Hence, the pressure drop decreases as bend-to-pipe radius ratio increases, which is an established fact for hydraulic pipelines [47]. It can be seen in the figure that the pressure drop variations within a bend with bend-to-pipe radius ratio of 8 resembles the one observed in the previous case i.e. the pressure drop increase upstream the capsule up to its front end, and then it constantly decreases until it coincides with the P'_{Bend} line. It can be further noticed that due to lesser curvature of the bend in the present case, the secondary flows are dissipated far downstream the capsule, and hence, the effect of the capsule is felt till $5d$ location downstream the capsule. K_{lc} has been computed to be 0.0661 in the present case, which is 11% lower than K_{lc} in the previous case, indicating lesser pressure drop contribution by the capsule.

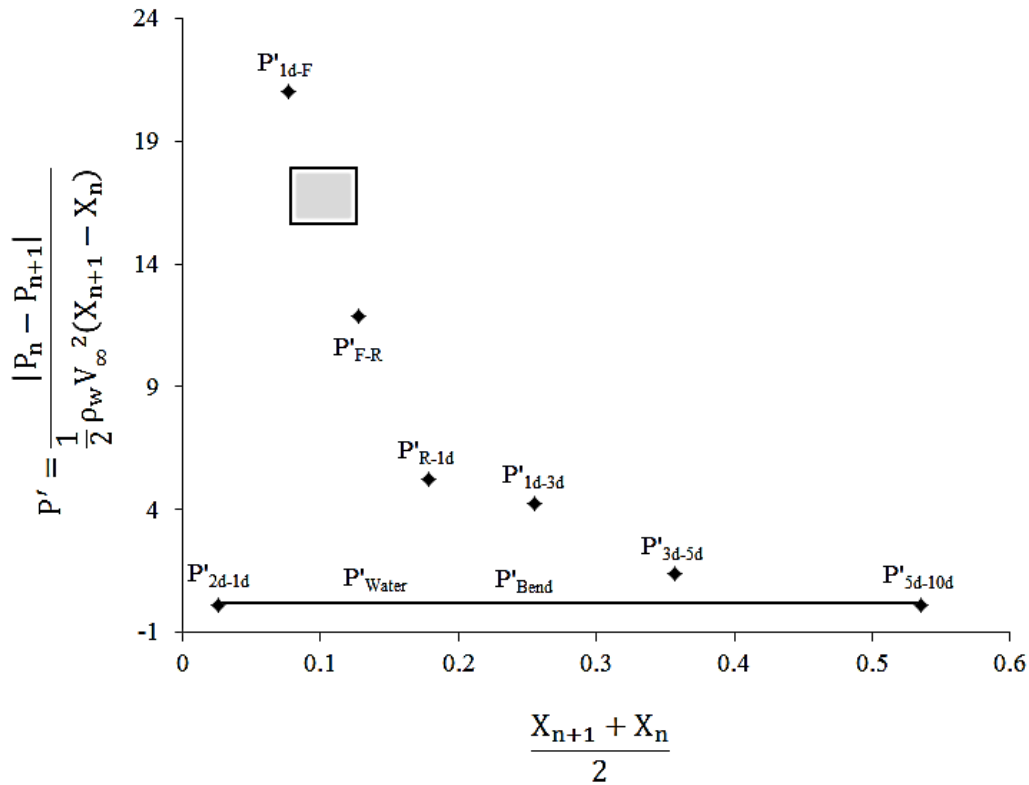


Figure 26 Variations in pressure drop across a horizontal HCP bend of $R/r=8$, for a single equi-density cylindrical capsule of $k=0.5$ and $Lc=1d$, at $V_{av}=1m/sec$

8.9 Novel Prediction Models for HCPs

Qualitative description of the static pressure distribution, along-with a new parameter to define losses in HCPs transporting cylindrical capsules has been discussed in detail in previous section. There is a need to develop semi-empirical expressions for the capsule friction factor and loss coefficient that can be fed into the design process of an HCP. Pressure drop predictions from validated CFD simulations have been used in order to develop novel semi-empirical prediction models for the capsule/s friction factor and loss-coefficient in HCPs. These prediction models have been developed using advanced statistical tools such as multiple regression analysis. The capsule friction factors and loss coefficients have been expressed as a function of the different geometrical and flow related parameters considered in the present study, in non-dimensional form. Table 7 summarises the developed prediction models for various cases.

Table 7 Friction Factors for Capsules in HCPs

Pipeline Orientation	Density of the Capsules	Pipe/Bend	fc and Klc Expressions
Horizontal	Equi-Density	Pipe	$f_c = \frac{\left(13.18 \left(\frac{N}{Lp} * Lc\right)^{0.178} k^{5.13} \frac{Lc^{0.1}}{d} \frac{Sc + Lp^{0.1}}{Lp}\right)}{Re_c^{0.117}}$

Heavy-Density	Bend	$K_{lc} = \frac{\left(691 \left(\frac{N}{Lp} * Lc \right)^{1.63} k^{2.92} \frac{Sc + Lp}{Lp}^{1.05} \right)}{Re_c^{0.026} \frac{R}{r}^{0.2} \frac{Lc}{d}^{1.88}}$	
	Pipe	$f_c = \frac{\left(3.38 \left(\frac{N}{Lp} * Lc \right)^{0.016} k^{5.24} \frac{Lc}{d}^{0.1} \frac{Sc + Lp}{Lp}^{0.1} \right)}{Re_c^{0.019}}$	
	Bend	$K_{lc} = \frac{\left(549 \left(\frac{N}{Lp} * Lc \right)^{0.5} k^{3.92} \right)}{Re_c^{0.14} \frac{Lc}{d}^{0.43} \frac{R}{r}^{0.2} \frac{Sc + Lp}{Lp}^{0.45}}$	
Vertical	Equi-Density	Pipe	$f_c = \frac{\left(6.3 \left(\frac{N}{Lp} * Lc \right)^{0.13} k^{4.96} \frac{Lc}{d}^{0.1} \frac{Sc + Lp}{Lp}^{0.1} \right)}{Re_c^{0.07}}$
		Bend	$K_{lc} = \frac{\left(10^{6.8} \left(\frac{N}{Lp} * Lc \right)^{1.22} k^{4.5} \frac{Sc + Lp}{Lp}^{1.35} \right)}{Re_c^{0.81} \frac{R}{r}^{0.2} \frac{Lc}{d}^{1.5}}$
		Pipe	$f_c = \frac{\left(4.16 \left(\frac{N}{Lp} * Lc \right)^{0.14} k^{4.8} \frac{Lc}{d}^{0.1} \frac{Sc + Lp}{Lp}^{0.1} \right)}{Re_c^{0.035}}$
Heavy-Density	Bend	$K_{lc} = \frac{\left(10^8 \left(\frac{N}{Lp} * Lc \right)^{1.33} k^{4.5} \frac{Sc + Lp}{Lp}^{1.35} \right)}{Re_c^{0.96} \frac{R}{r}^{0.2} \frac{Lc}{d}^{1.58}}$	

where Re_c is the Reynolds number of the capsule/s, which can be calculated as:

$$Re_c = \frac{\rho_c V_c d}{\mu} \quad (15)$$

All 373 numerical predictions regarding the pressure drop across HCPs have been used to develop the semi-empirical prediction models of table 7. In order to check the validity of these prediction models, f_c and K_{lc} from these models have been compared against CFD predicted f_c and K_{lc} values. An example of such a comparison is shown in figure 27 (for heavy-density cylindrical capsules in a horizontal straight pipe). It can be seen that more than 90% of the data points lie within $\pm 10\%$ error band.

9. Optimisation of HCPs

Optimisation of HCPs is vital for its commercial viability of transportation system. An optimisation model, based on Least-Cost Principle, has already been developed by the author in a previous study [32]. That optimisation model has been configured to work with the cylindrical capsules in the present study. The model is based on the least-cost principle, i.e. the pipeline transporting capsules is designed such that the total cost of the pipeline is minimum. The total cost of a pipeline transporting capsules consists of the manufacturing cost of the pipeline and the capsules plus the operating cost of the system.

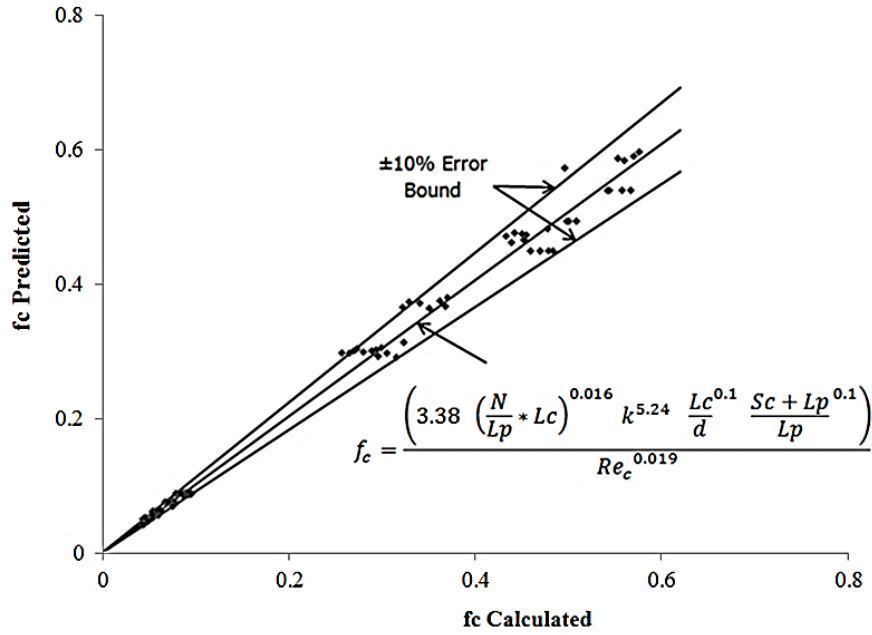


Figure 27 An example of comparison between computed and predicted capsule friction factors

$$C_{Total} = C_{Manufacturing} + C_{Operating} \quad (16)$$

The manufacturing cost can be further divided into the cost of the pipeline and the cost of the capsules. The operating cost refers to the cost of the power being consumed.

$$C_{Total} = C_{Pipe} + C_{Capsule} + C_{Power} \quad (17)$$

9.1 Cost of Pipes

The cost of pipe per unit weight of the pipe material is given by [48]:

$$C_{Pipe} = \pi D t \gamma_p C_2 L_p \quad (18)$$

where t is the thickness of the pipe wall. According to Davis and Sorenson [49], and Russel [50], the pipe wall thickness can be expressed as:

$$t = C_c D \quad (19)$$

where C_c is a constant of proportionality dependent on expected pressure and diameter ranges of the pipeline. Hence, the cost of the pipe becomes:

$$C_{Pipe} = \pi D^2 \gamma_p C_2 C_c L_p \quad (20)$$

9.2 Cost of Capsules

The cost of cylindrical capsules per unit weight of the capsule material can be calculated as [32]:

$$C_{Cylindrical\ Capsules} = \pi k D L_c t_c N \gamma_c C_3 \quad (21)$$

where t_c is the thickness of the capsule, N is the total number of capsules in the pipeline, L_c is the length of the capsule and γ_c is the specific weight of the capsule material.

9.3 Cost of Power

The cost of power consumption per unit watt is given by [30]:

$$C_{Power} = C_1 P \quad (22)$$

where P is the power requirement of the pipeline transporting capsules. It is the power that dictates the selection of the pumping unit to be installed. The power can be expressed as:

$$P = \frac{Q_m \times \Delta P_{Total}}{\eta} \quad (23)$$

where Q_m is the flow rate of the mixture, ΔP_{Total} is the total pressure drop in the pipeline transporting capsules and η is the efficiency of the pumping unit. Generally the efficiency of industrial pumping unit ranges between 60 to 75%. The total pressure drop can be calculated from the friction factor (and loss-coefficient) models developed.

9.4 Mixture Flow Rate

Liu reports the expression to find the mixture flow rate as [44]:

$$Q_m = \frac{\pi D^2}{4} V_{av} \quad (24)$$

for a circular pipe.

9.5 Total Pressure Drop

The total pressure drop in a pipeline can be expressed as a sum of the major pressure drop and minor pressure drop resulting from pipeline and pipe fittings respectively [33].

$$\Delta P_{Total} = \Delta P_{Major} + \Delta P_{Minor} \quad (25)$$

The major pressure drop can be expressed as follows for horizontal pipes as:

$$\Delta P_{Major} = f_w \frac{L}{D} \frac{\rho_w V_{av}^2}{2} + f_c \frac{L}{D} \frac{\rho_w V_{av}^2}{2} \quad (26)$$

and for vertical pipes as:

$$\Delta P_{Major} = f_w \frac{L}{D} \frac{\rho_w V_{av}^2}{2} + f_c \frac{L}{D} \frac{\rho_w V_{av}^2}{2} + \rho_w g \Delta h \quad (27)$$

Similarly, the minor pressure drop can be expressed as follows for horizontal bends as:

$$\Delta P_{Minor} = K_{lw} \frac{n \rho_w V_{av}^2}{2} + K_{lc} \frac{n \rho_w V_{av}^2}{2} \quad (28)$$

and for vertical bends as:

$$\Delta P_{Minor} = K_{lw} \frac{n\rho_w V_{av}^2}{2} + K_{lc} \frac{n\rho_w V_{av}^2}{2} + \rho_w g \Delta h \quad (29)$$

where n is the number of bends in the pipeline. Here, f_w can be found by the Moody's approximation as [45]:

$$f_w = 0.0055 + \frac{0.55}{Re_w^{\frac{1}{3}}} \quad (30)$$

K_{lw} has been found out to be:

$$K_{lw} = \frac{(3.05 - 0.0875 \frac{R}{r})}{Re_w^{\frac{1}{5}}} \quad (31)$$

9.6 Solid Throughput

The solid throughput, in m^3/sec , is the only input to the optimisation model developed here, which can be represented as [30]:

$$Q_c = \frac{\pi d^2 L_c}{4} \times \frac{\text{Number of capsules in the train}}{\text{Time taken to travel unit length}} \quad (32)$$

The number of capsules in the train are:

$$L_p = N L_c + (N - 1) S_c \quad (33)$$

where N is the number of capsules and can be represented as:

$$N = \frac{L_p + S_c}{L_c + S_c} \quad (34)$$

Hence:

$$Q_c = \frac{\pi d^2 L_c V_c}{4 L_p} \times \frac{L_p + S_c}{L_c + S_c} \quad (35)$$

Hence, V_c can be represented in terms of Q_c and V_{av} can be expressed in terms of V_c (using holdup expressions). Figure 28 depicts the flow chart of the optimisation model developed.

10. Design Example

Equi-density cylindrical capsules of $k=0.7$ need to be transferred from the processing plant to the storage area of the factory half kilometre away. The spacing between the capsules has been set at 3d. The required throughput is 1kg/sec. Find the optimal size of the pipeline and the pumping power required for this purpose.

Solution: According to the current market, the values of C_1 , C_2 , C_3 , and C_c are 1.4, 1.1, 0.95 and 0.01 respectively. Assuming the efficiency of the pumping unit to be 60%, and following the steps described in the working of the optimisation model, the following results (table 8) are obtained. It is noteworthy that the manufacturing cost is a one-off cost, whereas the cost of power consumption is an annual cost.

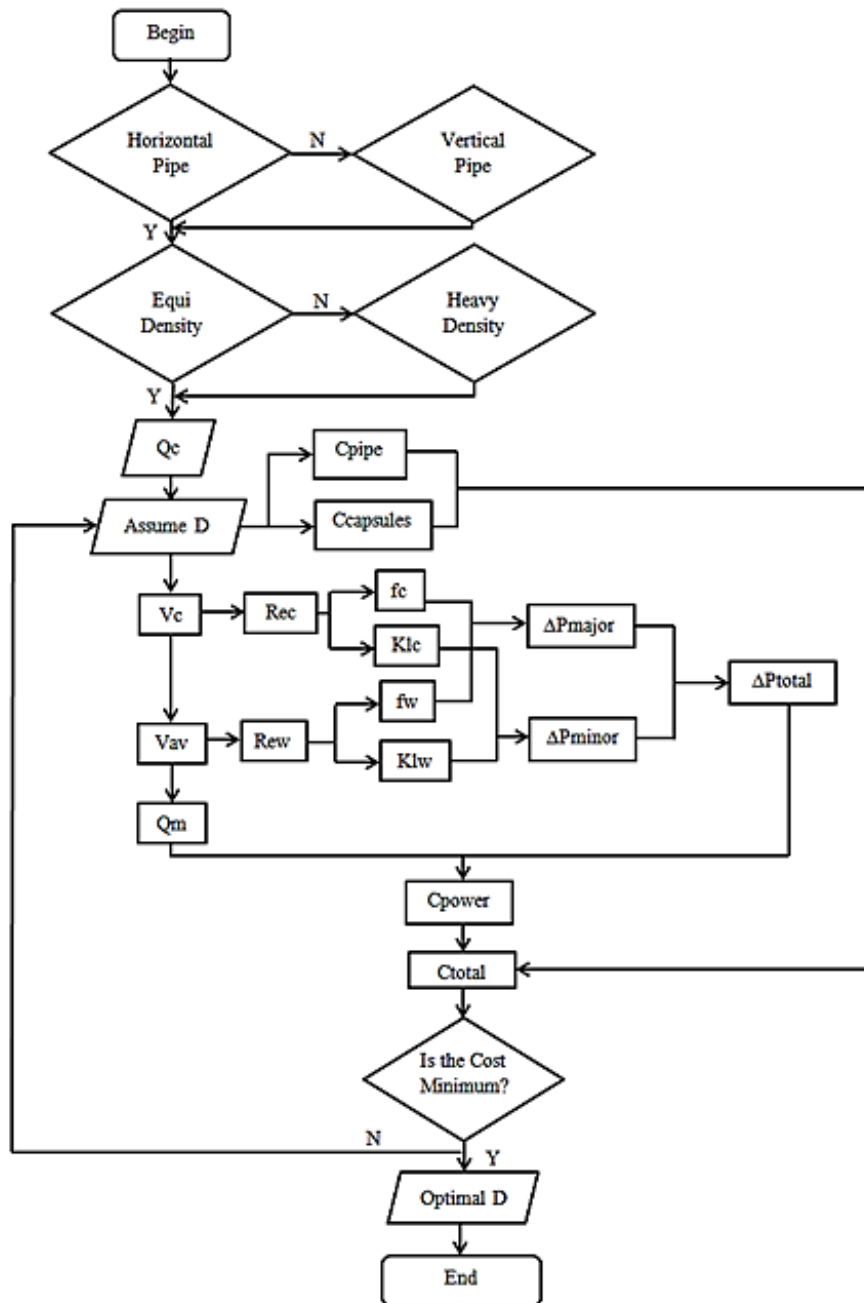


Figure 28 Flow chart of the optimisation methodology

Table 8 Variations in Pumping Power and Various Costs with respect to Pipeline Diameter

D	P	C _{Manufacturing}	C _{Power}	C _{Total}
(m)	(kW)	(£)	(£)	(£)
0.08	24.55	9129	34383	43512
0.09	13.83	11468	19362	30830
0.10	8.27	14073	11585	25658
0.11	5.20	16944	7280	24224
0.12	3.40	20081	4763	24844
0.13	2.30	23485	3225	26710
0.14	1.60	27154	2247	29401

The results presented in table 8 depict that a pipeline of diameter=110cm is optimum for the problem under consideration because the total cost for the pipeline is minimum at $D=0.11\text{m}$. The power of the pumping unit required, corresponding to the optimal diameter of the pipeline, is 5.2kW. It can be further seen that as the pipeline diameter increases, the manufacturing cost increases. This is due to the fact that pipes of larger diameters are more expensive than pipes of relatively smaller diameters. Moreover, as the pipeline diameter increases, the operating cost decreases. This is due to the fact that for the same solid throughput, increasing the pipeline diameter decreases the velocity of the flow within the pipeline. The operating cost has a proportional relationship with the velocity of the flow; hence, increase in the pipeline diameter decreases the operating cost of the pipeline.

11. Conclusions

From the result presented in the present study, it can be concluded that the presence of cylindrical capsule/s within a hydraulic pipeline alters the flow behaviour considerably and hence increases the pressure losses. Detailed analysis of the flow parameters' variations for different geometrical and flow configurations has revealed that the flow fields within an HCP vary significantly as the capsule concentration, size, density, flow velocity, pipe's inclination varies. Increase in capsule concentration and spacing increases the pressure drop within an HCP, while increasing the length of the capsule has marginal effects on the pressure drop. Furthermore, increase in capsule diameter increases the pressure drop across the pipeline. Heavier cylindrical capsules offer more resistance to the flow because of asymmetric and highly non-uniform flow behaviour within the HCPs, adding to the pressure losses. Similarly, increasing the average flow velocity increases the pressure drop across the pipeline; however the flow structure in the vicinity of the capsule remains the same.

It has also been observed that although the pressure drop across a vertical HCP is considerably higher as compared to a horizontal HCP, however, losses due to the capsule/s remain almost constant, and the primary contributing factor for pressure loss is the elevation of the pipeline. Moreover, it has been noticed that pressure drop across pipe bends is higher as compared to a straight pipeline, and increasing its R/r lowers the pressure drop across the pipe bend. A novel parameter has been developed that indicates the resultant pressure force acting on the capsule because of the relative velocity between the capsule and the flow. Based on the pressure drop results, novel semi-empirical prediction models have been developed for the friction factor/s and loss coefficient/s of the capsule/s, which have been embedded into a pipeline optimisation model that is based on least-cost principle. The optimisation model's only input is the solid throughput required from the HCP, while the primary output is the optimal pipeline diameter. A practical example has been included in order to demonstrate the usage and effectiveness of this optimisation model.

NOMENCLATURE

C_c	Constant of Proportionality (-)
C_1	Cost of Power consumption per unit Watt (£/W)
C_2	Cost of Pipe per unit weight of pipe material (£/N)
C_3	Cost of Capsules per unit weight of capsule's material (£/N)
c	Concentration of Solid Phase (%)
d	Diameter of Capsule/s (m)
D	Diameter of Pipe (m)
f	Darcy Friction Factor (-)
g	Acceleration due to gravity (m/sec^2)
h	Elevation (m)
H	Holdup (-)

k	Capsule to Pipe diameter ratio (-)
K_L	Loss Coefficient of Bends (-)
L	Length (m)
n	Number of Bends (-)
N	Number of Capsules (-)
P	Local Static Pressure (Pa)
Q	Flow Rate (m^3/sec)
R	Radius of Curvature of Pipe Bend (m)
r	Radius of Pipe (m)
Re	Reynolds Number (-)
s	Specific Gravity (-)
Sc	Spacing between the Capsules (m)
t	Thickness (m)
V	Velocity (m/sec)
X	X direction
Y	Y direction

GREEK SYMBOLS

Δ	Change
ε	Roughness Height of the Pipe (m)
η	Efficiency of the Pump (%)
μ	Dynamic Viscosity (Pa-sec)
π	Pi
ρ	Density (Kg/m^3)
γ	Specific Weight (N/m^3)

SUBSCRIPTS

av	Average
c	Capsule
F	Front
m	Mixture
p	Pipe
R	Rear
w	Water
∞	Free Stream

References

- [1] M. E. Charles, Theoretical Analysis of the Concentric Flow of Cylindrical Forms, Canadian Journal of Chemical Engineering, 41 (1962) 46–51.
- [2] H. S. Ellis, An Experimental Investigation of the Transport by Water of Single Cylindrical and Spherical Capsules with Density Equal to that of the Water, The Canadian Journal of Chemical Engineering, vol: 42 (1964) 1–8.
- [3] R. Newton, P. J. Redberger, G. F. Round, Numerical Analysis of Some Variables Determining Free Flow, Canadian Journal of Chemical Engineering, 42 (1963) 168–173.
- [4] H. H. Kroonenberg, A Mathematical Model for Concentric Horizontal Capsule Transport, Canadian Journal of Chemical Engineering, 57 (1979) 383.
- [5] Y. Tomita, M. Yamamoto, K. Funatsu, Motion of a Single Capsule in a Hydraulic Pipeline, Journal of Fluid Mechanics, 171 (1986) 495–508.

- [6] Y. Tomita, T. Okubo, K. Funatsu, Y. Fujiwara, Unsteady Analysis of Hydraulic Capsule Transport in a Straight Horizontal Pipeline, In the Proceedings of the 6th International Symposium on Freight Pipelines, Eds. H. Liu and G. F. Round, USA, (1989) 273–278.
- [7] C. W. Lenau, M. M. El-Bayya, Unsteady Flow in Hydraulic Capsule Pipeline, *Journal of Engineering Mechanics*, 122 (1996) 1168–1173.
- [8] M. F. Khalil, S. Z. Kassab, I. G. Adam, M. A. Samaha, Turbulent Flow around a Single Concentric Long Capsule in a Pipe, *Journal of Applied Mathematical Modelling*, 34 (2010) 2000–2017.
- [9] H. S. Ellis, An Experimental Investigation of the Transport in Water of Single Cylindrical Capsule with Density Greater than that of the Water, *Canadian Journal of Chemical Engineering*, (1964) 69–76.
- [10] J. Kruyer, P. J. Redberger, H. S. Ellis, The Pipeline Flow of Capsules, Part 9, *Journal of Fluid Mechanics*, 30 (1967) 513–531.
- [11] H. S. Ellis, Minimising the Pressure Gradients in Capsule Pipelines, *Canadian Journal of Chemical Engineering*, 52 (1974) 457–462.
- [12] J. Kruyer, W. T. Snyder, Relationship between Capsule Pulling Force and Pressure Gradient in a Pipe, *Canadian Journal of Chemical Engineering*, 53 (1975) 378–383.
- [13] V. C. Agarwal, M. K. Singh, R. Mishra, Empirical Relation for the Effect of the Shape of the Capsules and the Nose Shape on the Velocity Ratio of Heavy Density Capsules in a Hydraulic Pipeline, In the Proceedings of the Institute of Mechanical Engineers, Part E: *Journal of Process Mechanical Engineering*, (2001).
- [14] D. Barthes-Biesel, Capsule motion in flow: Deformation and Membrane Buckling, *C. R. Physique*, 10 (2009) 764–774.
- [15] D. Barthes-Biesel, Modelling the motion of Capsules in Flow, *Journal of Colloid & Interface Science*, 16 (2011) 3–12.
- [16] K. W. Chow, An Experimental Study of the Hydrodynamic Transport of Spherical and Cylindrical Capsules in a Vertical Pipeline, M. Eng. Thesis, McMaster University, (1979), Hamilton, Ontario, Canada.
- [17] L. Y. Hwang, D. J. Wood, D. T. Kao, Capsule Hoist System for Vertical Transport of Coal and Other Mineral Solids, *Canadian Journal of Chemical Engineering*, 59 (1981) 317–324.
- [18] B. Latto, K. W. Chow, Hydrodynamic Transport of Cylindrical Capsules in a Vertical Pipeline, *Canadian Journal of Chemical Engineering*, 60 (1982) 713–722.
- [19] M. Tachibana, Basic Studies on Hydraulic Capsule Transportation, Part 2, Balance and Start-up of Cylindrical Capsule in Rising Flow of Inclined Pipeline, *Bulletin of the JSME*, 26 (1983) 1735–1743.
- [20] A. Ohashi, K. Yanaida, The Fluid Mechanics of Capsule Pipelines, 1st Report, Analysis of the Required Pressure Drop for Hydraulic and Pneumatic Capsules, *Bulletin of JSME*, 29 (1986) 1719–1725.
- [21] K. Yanaida, M. Tanaka, Drag Coefficient of a Capsule Inside a Vertical Angular Pipe, *Powder Technology*, 94 (1997) 239–243.
- [22] P. K. Swamee, Capsule Hoist System for Vertical Transport of Minerals, *Journal of Transportation Engineering*, (1999) 560–563.
- [23] P. Vlasak, J. Myska, The Effect of Pipe Curvature on the Flow of Carrier Liquid Capsule Train System, In the Proceedings of the Institute of Hydrodynamics, (1983) Praha.
- [24] P. Vlasak, V. Berman, A Contribution to Hydro-transport of Capsules in Bend and Inclined Pipeline Sections, *Handbook of Conveying and Handling of Particulate Solids*, (2001) 521–529.

- [25] H. G. Polderman, (1982) Design Rules for Hydraulic Capsule Transport Systems, *Journal of Pipelines*, 3 (1982) 123–136.
- [26] M. Assadollahbaik, H. Liu, Optimum Design of Electromagnetic Pump for Capsule Pipelines, *Journal of Pipelines*, 5 (1986) 157–169.
- [27] P. K. Swamee, Design of Sediment Transporting Pipeline, *Journal of Hydraulic Engineering*, 121 (1995).
- [28] V. C. Agarwal, R. Mishra, Optimal Design of a Multi-Stage Capsule Handling Multi-Phase Pipeline, *International Journal of Pressure Vessels and Piping*, 75 (1998) 27–35.
- [29] Y. Sha, X. Zhao, Optimisation Design of the Hydraulic Pipeline Based on the Principle of Saving Energy Resources, In the Proceedings of Power and Energy Engineering Conference (2010) Asia-Pacific.
- [30] T. Asim, R. Mishra, Optimal Design of Hydraulic Capsule Pipeline Transporting Spherical Capsules, *Canadian Journal of Chemical Engineering*, In Press, (2015).
- [31] Darcy, H. *Recherches Expérimentales Relatives au Mouvement de l'Eau dans les Tuyaux* [Experimental Research on the Movement of Water in Pipes], Mallet-Bachelier (1857) Paris.
- [32] T. Asim, , Computational Fluid Dynamics based Diagnostics and Optimal Design of Hydraulic Capsule Pipelines, Ph.D. Thesis, University of Huddersfield, (2013), Huddersfield, U.K.
- [33] B. R. Munson, D. F. Young, T. H. Okiishi, *Fundamentals of Fluid Mechanics*, John Wiley & Sons Inc., 4th ed., U.S.A. 2002.
- [34] D. Ulusarlan, I. Teke, An Experimental Investigation of the Capsule Velocity, Concentration Rate and the Spacing between the Capsules for the Spherical Capsule Train Flow in a Horizontal Circular Pipe, *Journal of Powder Technology*, 159 (2005) 27–34.
- [35] Industrial Accessories Company accessible at <http://www.iac-intl.com/parts/PB103001r2.pdf>
- [36] S. A. Morsi, A. J. Alexander, An Investigation of Particle Trajectories in Two-Phase Flow Systems, *Journal of Fluid Mechanics*, 55 (1972) 193–208.
- [37] D. Ulusarlan, Effect of Capsule Density and Concentration on Pressure Drops of Spherical Capsule Train Conveyed by Water, *Journal of Fluids Engineering*, 132 (2009).
- [38] C. Ariyaratne, Design and Optimisation of Swirl Pipes and Transition Geometries for Slurry Transport, Ph.D. Thesis, (2005), The University of Nottingham.
- [39] M. Rosenfeld, E. Rambod, M. Gharib, Circulation and formation number of laminar vortex rings, *Journal of Fluid Mechics*, 376 (1998) 297-318.
- [40] K. Mohseni, M. Gharib, A model for universal time scale of vortex ring formation, *Physics of Fluids*, 10 (1998) 2436-2438.
- [41] M. Gharib, E. Rambod, K. Shariff, A Universal Time Scale for Vortex Ring Formation, *Journal of Fluid Mechanics*, 360 (1998) 121-140.
- [42] M. Shusser, M. Gharib, Energy and Velocity of a Forming Vortex Ring, *Physics of Fluids*, 12 (2002) 618-621.
- [43] J. Feng, P. Y. Huang, D. D. Joseph, Dynamic Simulation of the Motion of Capsules in Pipelines, *Journal of Fluid Mechanics*, 286 (1995) 201-227.
- [44] H. Liu, *Pipeline Engineering*, CRC Press, U.S.A. 2003.
- [45] L. F. Moody, Friction factors for Pipe Flow, *Transactions of the ASME*, 66 (1944) 671-684.
- [46] R. Mishra, S. N. Singh, V. Seshedri, Study of Wear Characteristics and Solid Distribution in Constant Area and Erosion-Resistant Long-Radius Pipe Bends for the flow of Multisized Particulate Slurries, *Wear*, 217 (1998) 297–306.
- [47] U. Kumar, R. Mishra, S. N. Singh, V. Seshadri, Effect of particle gradation on flow characteristics of ash disposal pipelines, *Powder Technology*, 132 (2003) 39-51.

- [48] P. N. Cheremisinoff, S. I. Cheng, Civil Engineering Practice, Technomies Publishing Co., U.S.A., 1988.
- [49] C. Davis, K. Sorensen, Handbook of Applied Hydraulics, McGraw-Hill Book Co., 3rd ed., U.S.A., 1969.
- [50] G. Russel, Hydraulics, Holt, Rinehart and Winston, 5th ed., U.S.A., 1963.